



Master Thesis

Optimization of current sensors with Hall probe and Rogowski coil

Study programme:

N0714A150003 Mechatronics

Study branch:

N0714A150003MEA / Mechatronics

Author:

Kaushal Singara Chari

Supervisor:

Ing. Miroslav Novak

Institute of Mechatronics and Technical informatics

Liberec 2022



Master Thesis Assignment Form

Optimization of current sensors with Hall probe and Rogowski coil

<i>Name and surname:</i>	Kaushal Singara Chari
<i>Identification number:</i>	M2100029
<i>Study programme:</i>	N0714A150003 Mechatronics
<i>Study branch (specialization):</i>	N0714A150003MEA / Mechatronics
<i>Assigning department:</i>	Institute of Mechatronics and Technical informatics
<i>Academic year:</i>	2022/2023

Rules of Elaboration:

1. The goal is to optimize the design of a current sensor based on Hall sensors without a magnetic circuit and, in the second variant, on a Rogowski coil. Make a literature search on the principle of current sensors with a Hall probe and a Rogowski coil, focusing on inaccuracies caused by geometric asymmetry.
2. Create a sensor model and perform finite element simulations of the effect of geometric inaccuracies. The use of the freely available FEMM environment or university license ANSYS/COMSOL or similar SW is assumed.
3. The goal is to determine the influence of the primary conductor position, the effect of the surrounding magnetic fields from the nearby conductors outside the own sensor, and the impact of the geometric manufacturing inaccuracies of the own sensor on the output signal, i.e., the measured current.

Scope of Graphic Work: by appropriate documentation
Scope of Report: 40–50 pages
Thesis Form: printed/electronic
Thesis Language: English

List of Specialised Literature:

- [1] DJOKIĆ, Branislav, 2009. The Design and Calibration of Rogowski Coils. NCSLI Measure [online]. 4(2), 62–75. ISSN 1931-5775, 2381-0580. Available from: doi:10.1080/19315775.2009.11721474
- [2] UMAŃSKI, Sławomir, 2011. Handbook of magnetic measurements. Boca Raton: Taylor & Francis. Series in sensors. ISBN 978-1-4398-2951-6.

Thesis Supervisor: Ing. Miroslav Novak
Institute of Mechatronics and Technical informatics

Date of Thesis Assignment: October 12, 2022
Date of Thesis Submission: August 29, 2023

Zdeněk Plíva
Dean

S.S.

Josef Černohorský
Head of institute

Declaration

I hereby certify, I, myself, have written my master thesis as an original and primary work using the literature listed below and consulting it with my thesis supervisor and my thesis counsellor.

I acknowledge that my master thesis is fully governed by Act No. 121/2000 Coll., the Copyright Act, in particular Article 60 – School Work.

I acknowledge that the Technical University of Liberec does not infringe my copyrights by using my master thesis for internal purposes of the Technical University of Liberec.

I am aware of my obligation to inform the Technical University of Liberec on having used or granted license to use the results of my master thesis; in such a case the Technical University of Liberec may require reimbursement of the costs incurred for creating the result up to their actual amount.

At the same time, I honestly declare that the text of the printed version of my master thesis is identical with the text of the electronic version uploaded into the IS STAG.

I acknowledge that the Technical University of Liberec will make my master thesis public in accordance with paragraph 47b of Act No. 111/1998 Coll., on Higher Education Institutions and on Amendment to Other Acts (the Higher Education Act), as amended.

I am aware of the consequences which may under the Higher Education Act result from a breach of this declaration.

29th August, 2023.

{Date of declaration}

Kaushal Singara Chari

Optimization of current sensors with Hall probe and Rogowski coil

Abstract

The main aim of this thesis is to understand the working of 2 magnetic current sensors, the Rogowski coil and Hall sensor, and study the errors induced in these sensors due to geometrical asymmetries and changes in the position of the primary conductor. We created 2 mathematical models based on known analytical formulae to estimate the error in measurement due to the gap for the PCB Rogowski coil and the split core Rogowski coil for different positions of the primary conductor. The gap creates asymmetries in the geometry of the coil and the model showed that there is a drop in the induced voltage if the primary conductor is placed close to the gap and the voltage induced in the coil is found to higher if an external current carrying wire is placed close to the gap. We also created a mathematical model to estimate the error induced in Hall sensor due to changes in the position of the primary conductor based on the number of sensing elements surrounding the conductor. The model shows that the impact of primary conductor position can be reduced by increasing the number of sensing elements around the conductor. These models were validated by comparing the results to equivalent finite element models and also by measuring the error with some physical experiments.

Keywords

Faraday's law of electromagnetic induction, Biot-Savart's law, Hall effect, mathematical modelling, finite element modelling.

Acknowledgements

First and foremost, I would like to thank my project supervisor Ing. Miroslav Novak who has guided me through every step of this project. I would also like to thank Ing. Jakub Eichler for his support with Ansys maxwell software. Lastly, I would also like to than my parents for always supporting me with everything.

Contents

- Introduction 1**
 - 1.1 Direct (shunt based) current sensing..... 1
 - 1.2 Indirect (magnetic) current sensing 2
 - 1.3 Significance of error estimation: 5
- Rogowski coil 6**
 - 2.1 Error study of Rogowski coil..... 7
 - 2.2 Error approximation of PCB coil with single gap 8
 - 2.2.1 With the help of analytical formulae: 8
 - 2.2.2 By finite element modelling..... 11
 - 2.2.3 Experimental measurement of error..... 26
 - 2.3 Error approximation of split core Rogowski coil 29
 - 2.3.1 With the help of analytical formulae..... 29
 - 2.3.2 By finite element modelling..... 31
 - 2.3.3 Experimental measurement of error..... 36
- Hall sensor..... 38**
 - 3.1 Error study of Hall sensor 40
 - 3.1.1 Estimation of error using analytical formulae 41
 - 3.1.2 Estimation of error by finite element model 46
 - 3.1.3 Experimental measurement of error 48
- Conclusion..... 49**
- References 51**
- List of Attachments 52**

List of Images

Figure description	Pg No.
Figure 1.1: Direct current sensing method [5]	1
Figure 1.2: Magnetic current sensing method [5]	2
Figure 1.3: Diagram to calculate magnetic field at a given point [8].	3
Figure 1.4: Types of magnetic field sensors [4]	4
Figure 2.10: Rogowski coil [6]	6
Figure 2.11: PCB coil with single gap	7
Figure 2.12: Split core Rogowski coil	8
Figure 2.13: Arc created with mean radius and given gap	12
Figure 2.14: Measuring the gap ($\approx 5.4^0$)	12
Figure 2.15: Ring created using sweep command	13
Figure 2.16: 2nd sweep	13
Figure 2.17: Relationship between sd6 and sweep	14
Figure 2.18: Intersection between the swept surfaces	14
Figure 2.19: Sweep along the intersection	15
Figure 2.20: Coil without reference surfaces	15
Figure 2.21: Coil terminals	16
Figure 2.22: Coil in fusion 360	16
Figure 2.23: Final coil	17
Figure 2.24: Coil with the conductor in centre	17
Figure 2.25: Ansys Maxwell G.U.I.	18
Figure 2.26: Specifying solution type	18
Figure 2.27: Material selection window	19
Figure 2.28: Region of analysis	19
Figure 2.29: Applying current to the first winding	20
Figure 2.30: Coil terminal	20
Figure 2.31: Direction of coil terminals for primary conductor	21
Figure 2.32: Direction of coil terminals for Rogowski coil	21
Figure 2.23: Setting surface approximation	22
Figure 2.34: Selecting surface for TAU meshing	22
Figure 2.35: Solution setup	22
Figure 2.36: Saving the solution at every time step	23
Figure 2.37: Specifying the required result	23
Figure 2.38: Primary conductor moved near the gap	24
Figure 2.39: Schematic diagram of experiment	26
Figure 2.40: C.N.C. bench used for positioning the conductor	26
Figure 41: Complete setup of the experiment	27
Figure 2.42: Geometric representation of split core Rogowski coil	31
Figure 2.43: Creating second half using mirror command	32
Figure 2.44: Mirror plane	32
Figure 2.45: Final geometry for analysis	33

Figure 2.46: Coil terminals for winding	33
Figure 2.47: Coil terminals for winding 2	34
Figure 2.48: Coil terminals for winding 3	34
Figure 2.49: Conductor moved near gap	35
Figure 2.50: Split core coil mounted on the C.N.C. bench	36
Figure 3.10: Hall effect	39
Figure 3.11: Hall sensor with multiple sensing elements	41
Figure 3.12: Equivalent schematic diagram	41
Figure 3.13: Geometry for analysis	46
Figure 3.14: Total flux through the given 4 surfaces	47
Figure 3.15: Conductor moved away from the centre	47
Figure 3.16: Total flux for displaced conductor	47
Figure 3.17: Hall sensor with 4 sensing elements mounted on the C.N.C bench	48
Figure 3.18: Hall sensor used for the experiment	48

List of graphs

Graph	Pg No.
Graph 2.11: Gap v/s Displacement v/s Error	10
Graph 2.12: Distance v/s Gap v/s Induced voltage	11
Graph 2.13: Induced voltage when the primary conductor is in the centre	24
Graph 2.14: Induced voltage when the primary conductor is near the gap	25
Graph 2.15: Primary current (peak to peak)	27
Graph 2.16- Induced voltage (peak to peak)	28
Graph 2.17: V_{RMS} of induced voltage	28
Graph 2.18: Error induced due to gap	29
Graph 2.19: Error due to gap in split core Rogowski coil	30
Graph 2.20: Induced voltage due to conductor near gap	31
Graph 2.21: Induced voltage in the 2 windings when the conductor is in the centre	34
Graph 2.22: Voltage induced in each winding when the conductor is near the gap	35
Graph 2.23: Primary current measured at different primary conductor positions (peak to peak)	36
Graph 2.24: Induced voltage measured at different primary conductor positions (peak to peak)	37
Graph 2.25: Root mean square voltage calculated at different positions of the primary conductor	38
Graph 2.26: Error calculated for different position of the primary conductor	38
Graph 3.11 Conductor displacement v/s number of sensing elements	43
Graph 3.12: Alpha v/s number of sensing elements v/s error	44
Graph 3.13: Conductor displacement (d+R) v/s no. of sensing elements v/s net flux	45
Graph 3.14: Induced voltage measure at different distances from the centre	49

List of Symbols

\vec{B}	Magnetic field (T).
\vec{E}	Electric field (V/m).
Φ	Magnetic flux (Wb).
I	Current(A).
V	Electric potential difference (V).
\vec{v}	Velocity (m/s).
\vec{F}	Force (N).
q	Charge (C) .
M	Co-efficient of Mutual Inductance.
μ_0	Permeability of free space (H/m).
\vec{r}	Perpendicular distance between primary conductor and sensing element.
\vec{ds}	Area vector normal to surface.
\vec{dL}	Small vector tangential to the path.
ϵ	Error
ϵ_V	Induced voltage in Rogowski coil
ϵ_H	Induced voltage in Hall sensor.
w	Thickness of sensor
Θ	Angle between surface Normal and magnetic field
g	Gap in Rogowski coil.
d	Displacement of conductor.
R	Outer radius of the sensor
r	Inner radius of the sensor.
N	Number of turns in Rogowski coil/ number of sensing elements in Hall sensor.

List of tables

Table description	Pg. No.
Table 1.1: Accuracy classes of current sensors	5
Table 4.1: Summary of results	49

Introduction

An electric current is a flow of charged particles, such as electrons or ions, moving through an electrical conductor or space. It is defined as the net rate of flow of electric charge through a surface. The moving particles are called charge carriers, which may be one of several types of particles, depending on the conductor. In electric circuits the charge carriers are often electrons moving through a wire. In semiconductors they can be electrons or holes. In an electrolyte the charge carriers are ions, while in plasma, an ionized gas, they are ions and electrons. The SI unit of electric current is the ampere, or amp, which is the flow of electric charge across a surface at the rate of one coulomb per second. The ampere (symbol: A) is SI unit of current [3]. In most circuits the charge carries are electrons with a charge of $1.602 \times 10^{-19} \text{C}$. therefore, if a current of 1A flows through a conductor, it means that $1/1.602 \times 10^{-19} \approx 6.242 \times 10^{18}$ electrons will flow through the cross section of a conductor in 1 second.

It is impossible to directly count the number of electrons flowing through the cross section of the conductor. Hence, current flowing through a conductor is estimated by measuring other physical quantities (magnetic field or voltage) which have a clearly defined mathematical relationship with the amount of current flowing through the conductor. Based on the physical quantity used to estimate the amount of current flowing through the conductor, current measurement is classified into 2 categories, direct (shunt-based) current sensing and indirect (magnetic) current sensing.

1.1 Direct (shunt based) current sensing

The direct current sensing method is explained in the figure below.

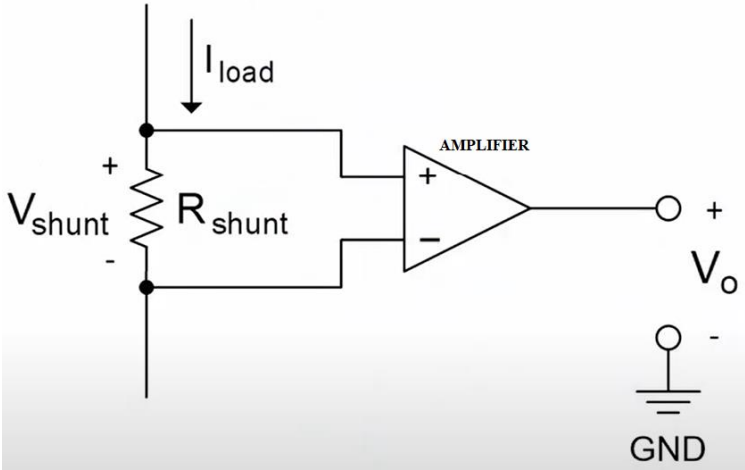


Figure 1.1: Direct current sensing method [5]

The direct current sensing method is based on ohm's law ($V = IR$). The current to be measured is sent through a shunt resistor of known resistance and the voltage drop across the resistor is measured. This value is substituted in the equation of ohm's law and the equation is solved to find the value of current. even though this method of current sensing yields very precise and accurate results, it has the following disadvantages:

- Some energy is lost as the current flows through the shunt resistor.
- The sensing circuitry needs to be directly connected to the monitored system, which may not always be possible.
- Low dynamic range of current measurement.

To overcome these disadvantages indirect (magnetic) current sensing method is used.

1.2 Indirect (magnetic) current sensing

The magnetic current sensing method is shown in the figure below:

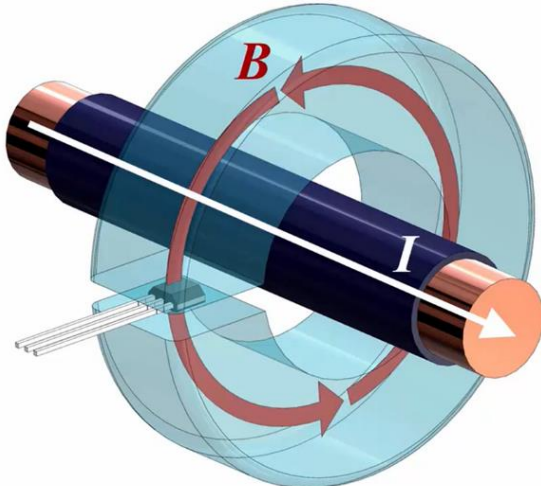


Figure 1.2: Magnetic current sensing method [5]

The magnetic current sensing method uses the magnetic field created by the current carrying conductor to estimate the current in the conductor. It is based on Biot Savart law.

Biot Savart law states that the magnetic field due to a tiny current element at any point is proportional to the length of the current element, the current, the sine of the angle between the current direction and the line joining the current element and the point, and inversely proportional to the square of the distance of that point. It can be represented mathematically by the equation below:

$$\vec{dB} = \frac{\mu_0}{4\pi} * \frac{i(\vec{dl} \times \vec{r})}{r^3} \quad (1.1)$$

Where, \vec{dl} is a tiny vector in the direction of current.

\vec{r} is a vector between the tiny current element and the point at which the magnetic is to be calculated.

\vec{dB} is the magnetic field at the point.

i is the current flowing through the element.

μ_0 is the coefficient of permeability ($= 4\pi * 10^{-7}$ H/m for free space).

Magnetic permeability is defined as the ratio of the magnetic induction to the magnetic intensity. It is a scalar quantity and is denoted by the symbol μ . Magnetic permeability helps us measure a material's resistance to the magnetic field or measure the degree to which a magnetic field can penetrate through a material [9].

Eq. (1.1) can be re-written in scalar form as shown below.

$$dB = \frac{\mu_0 i * dl * r * \sin(\theta)}{4\pi * r^3} = \frac{\mu_0 i * dl * \sin(\theta)}{4\pi * r^2} \quad (1.2)$$

From eq. (1.2), it is possible to find the strength of magnetic field due to a straight wire as shown below.

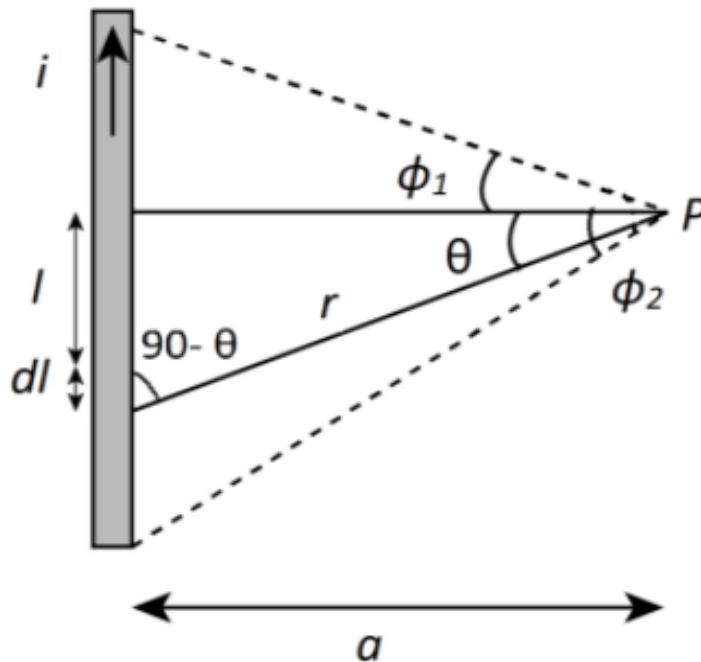


Figure 1.3: Diagram to calculate magnetic field at a given point [8].
note that ϕ_1 and ϕ_2 are measured in opposite directions.

applying Bio- savart's law, the magnetic field due to the current element dl at point P is,

$$dB = \frac{\mu_0 i * dl * \sin(90 - \theta)}{4\pi * r^2} \quad (1.3) \quad \because \theta \text{ is angle between } \vec{dl} \text{ \& } \vec{r}.$$

$$r = \frac{a}{\cos(\theta)} \text{ where } a \text{ is the perpendicular distance of point P from the wire.}$$

$$l = a \tan(\theta).$$

$$\therefore \frac{dl}{d\theta} = a \sec^2 \theta \Rightarrow dl = a \sec^2 \theta d\theta$$

Substituting the value of r and dl in eq. (1.3);

$$dB = \frac{\mu_0 i * a \sec^2 \theta d\theta * \sin(90-\theta)}{4\pi * (a/\cos(\theta))^2} = \frac{\mu_0 i d\theta \cos \theta}{4\pi a}$$

Integrating from ϕ_1 to ϕ_2 ;

$$B = \int_{-\phi_1}^{\phi_2} dB = \int_{-\phi_1}^{\phi_2} \frac{\mu_0 i \cos \theta}{4\pi a} d\theta = \frac{\mu_0 i}{4\pi a} (\sin(\phi_2) + \sin(\phi_1)) \quad (1.4)$$

Assuming that the wire is of reasonably long length, $\phi_1 \approx \phi_2 \approx 90^\circ$, we get;

$$|\vec{B}| = \frac{\mu_0 i}{2\pi a} \quad (1.5)$$

From the above equation, it can be seen that it is possible to estimate the amount of current in a conductor by measuring the intensity of magnetic field at a particular distance from the current carrying conductor. The sensors that are commonly used to measure the magnetic field around a current carrying conductor are listed in the flowchart below.

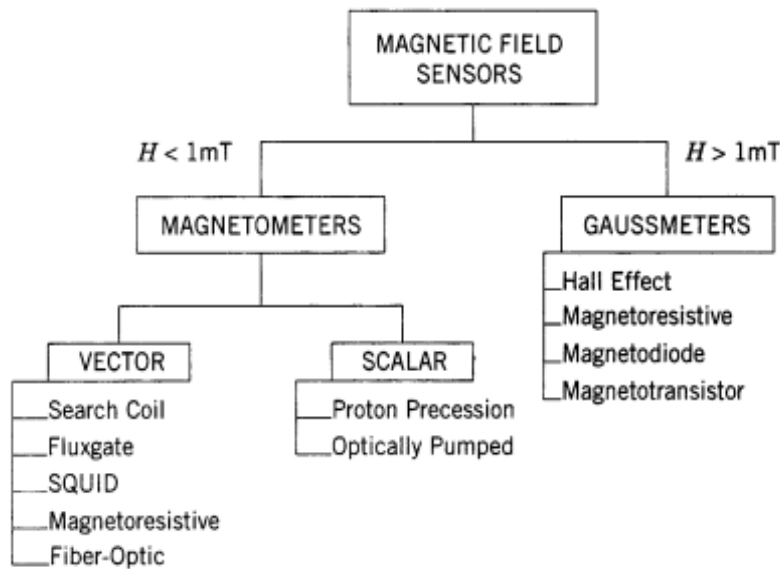


Figure 1.4: Types of magnetic field sensors [4]

Another important sensor which is used to measure a.c. current is the Rogowski coil, that works based on Biot Savart's law & faraday's law of electromagnetic induction. As we can see from the above derivation, the magnetic field intensity at any given point due to a current carrying wire depends on a lot of geometric parameters. Any change in these parameters will change the strength of the magnetic field which could result in an error during current measurement. In our project we have studied the Rogowski coil and Hall sensor in detail, and determined the error induced in the measurement of current due to a change in certain geometrical parameters like the positioning of the current carrying wire, or the geometrical design of these sensors.

1.3 Significance of error estimation:

Current measurement is commonly done for two reasons:

- As part of energy measurement which is used for pricing.
- Operational measurements and current protection used to check and the proper working of electronic appliances and ensuring that the current is under safe and permissible limits.

Sensors used for measuring current as part of energy measurement are expected to be extremely accurate as even small errors of 1-2% can add up over a huge number of customers and result in big losses for the company. Sensors used for operational measurements can be allowed to be less accurate as most appliances are designed to tolerate small changes in current. The requirements for accuracy, for different current sensors is specified by the international electrotechnical commission (I.E.C). The accuracy requirements for Hall sensors and Rogowski coils are specified by the standards IEC 61869-1, IEC 61869-6, IEC 61869-10, pro DC IEC 61869-14. Based on the accuracy of sensors, they are also classified into different accuracy classes as shown below.

Table 1.1: Accuracy classes of current sensors

Accuracy class	Ratio error $\varepsilon, \varepsilon_{cor1}$					\pm phase error at primary current shown below									
	\pm %					Minutes					Centiradians				
	at current					at current					at current				
	$0,01 I_{pr}$	$0,05 I_{pr}$	$0,2 I_{pr}$	I_{pr}	$K_{p_{cr}} \times I_{pr}$	$0,01 I_{pr}$	$0,05 I_{pr}$	$0,2 I_{pr}$	I_{pr}	$K_{p_{cr}} \times I_{pr}$	$0,01 I_{pr}$	$0,05 I_{pr}$	$0,2 I_{pr}$	I_{pr}	$K_{p_{cr}} \times I_{pr}$
0,1	-	0,4	0,2	0,1	0,1	-	15	8	5	5	-	0,45	0,24	0,15	0,15
0,2	-	0,75	0,35	0,2	0,2	-	30	15	10	10	-	0,9	0,45	0,3	0,3
0,2 S	0,75	0,35	0,2	0,2	0,2	30	15	10	10	10	0,9	0,45	0,3	0,3	0,3
0,5	-	1,5	0,75	0,5	0,5	-	90	45	30	30	-	2,7	1,35	0,9	0,9
0,5 S	1,5	0,75	0,5	0,5	0,5	90	45	30	30	30	2,7	1,35	0,9	0,9	0,9
1,0	-	3,0	1,5	1,0	1,0	-	180	90	60	60	-	5,4	2,7	1,8	1,8
3	-	-	4,5	3	3	-	-	-	-	-	-	-	-	-	-

Normally, current sensors used for pricing are expected to have an error of 0.2 to 0.5% while the sensors used for operational measurements are around 1 to 3%. based on the purpose of measurement, a sensor of required accuracy class is selected. Since, the accuracy of magnetic sensors can be affected by geometric parameters or surrounding magnetic fields, it is important to estimate the error that might be induced due to these factors and ensure that the sensor is designed in such a way, that the error is always within permissible limits. Our project contributes to this goal by estimating these errors for some assumed measuring conditions and shows how this error is expected to change, for different positions of the primary conductor or for some specific changes in the design of the sensor.

Rogowski coil

The Rogowski coil is a passive transducer used for measuring alternating current. It is named after German physicist Walter Rogowski (7 May 1881 – 10 March 1947), who designed it for the measurement of a.c. current. It is an inductor coil that can be easily coiled around a current carrying conductor. It is capable of measuring large currents of several thousand amperes. A simplified image of the Rogowski coil is shown in the figure below.

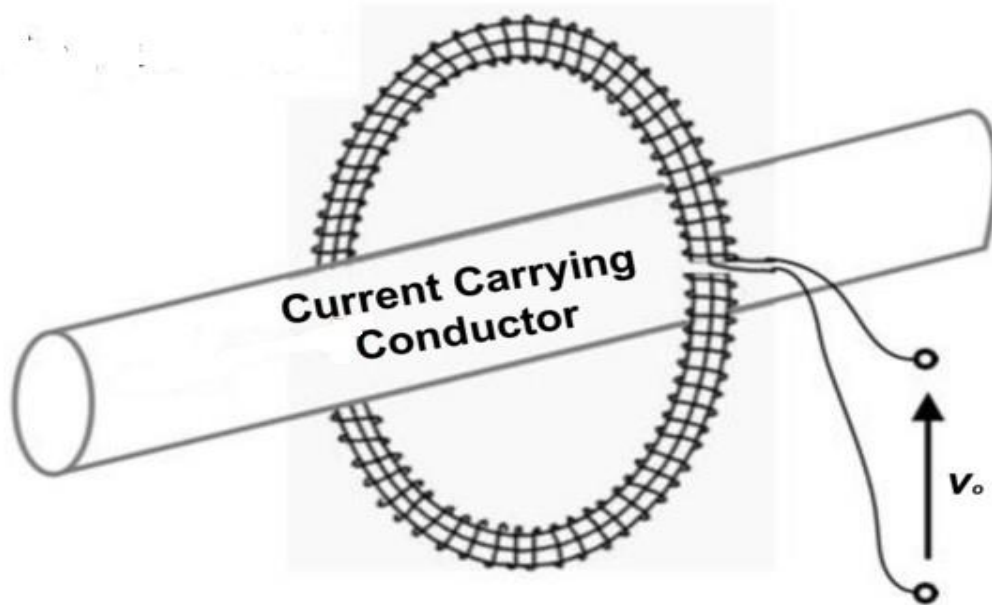


Figure 2.10: Rogowski coil [6]

It works based in biot-Savart's and *Faraday's law of electromagnetic induction*. Electromagnetic induction is defined as the production of an electromotive force (e.m.f.), across an electrical conductor when it is placed in a changing magnetic field. Faraday's law states that this induced e.m.f is equal to the rate of change of magnetic flux flowing through the coil. It can be written mathematically by the equation below.

$$\mathcal{E}_V = -\frac{d\phi_T}{dt} = -M \frac{di_p}{dt} \quad (2.10)$$

Were, \mathcal{E}_V is the induced voltage.

ϕ_T is the total magnetic flux flowing through the coil.

i_p is the current flowing in the primary coil. (i.e., the wire whose current is to be measured).

M is the coefficient of *mutual inductance*.

The coefficient of mutual inductance is defined as the amount of e.m.f. induced in the secondary when the rate of change of current in the primary 1A/sec. Its SI unit is Henry(H). $1H = \frac{1\text{volt} \cdot 1\text{sec}}{1A}$. It depends on the geometrical factors like the radius of coil, separation between

primary & secondary, orientation of the coils etc. The negative sign in eq. (2.10) indicates that the current flowing in the conductor due to this induced voltage will create a magnetic field that opposes the change in the magnetic flux. This direction of magnetic field is derived by using *lenz's law* [7] which is based on the law of conservation of energy.

2.1 Error study of Rogowski coil

Since the coefficient of mutual inductance is based on geometric parameters, it is bound to change if there is any change in the position of the primary conductor. Reports related to the design and accuracy of Rogowski coils have always highlighted that these changes can be reduced to negligible values, if the coil is perfectly symmetric from all directions [10][11][12]. One of the common causes of asymmetry in Rogowski coils is the gap between the start and end of the windings or the gap between 2 windings in a split core Rogowski coils. These two types of coils are shown in the figures below.

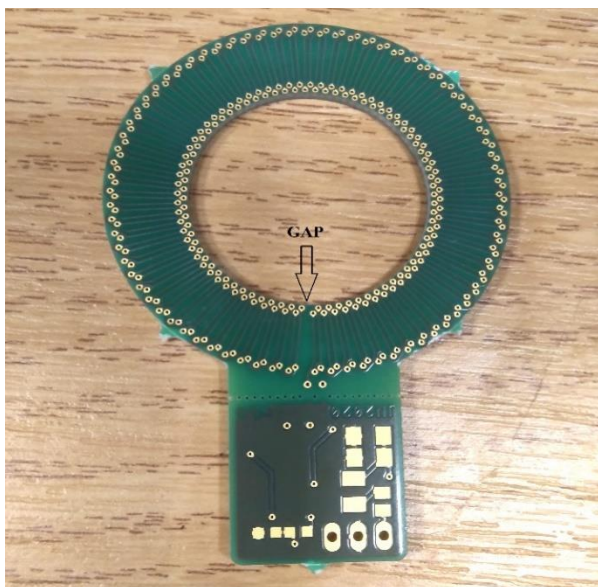


Figure 2.11: PCB coil with single gap

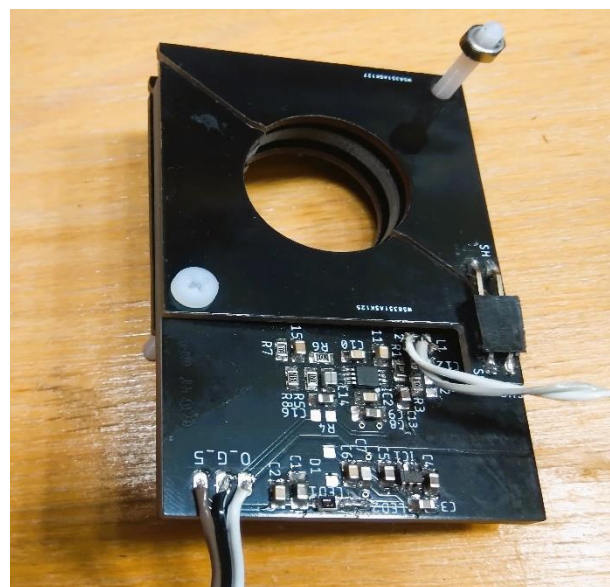


Figure 2.12: Split core Rogowski coil

In this project, we have estimated the errors induced in these coils during measurements due to these gaps. We have estimated this error in the following 3 ways:

1. With the help of analytical formulae.
2. Finite element modelling.
3. Physical experiments.

2.2 Error approximation of PCB coil with single gap

2.2.1 With the help of analytical formulae:

We can see that it is not possible to analytically calculate these errors using eq. (2.10) as it does not include any geometrical parameters that affect the coefficient of mutual inductance. Faraday's law was mathematically re-written by Scottish physicist Mr. James Clerk Maxwell (13 June 1831 – 5 November 1879) in integral and differential form as shown below.

$$\oint_c \vec{E} \cdot d\vec{L} = -\frac{d}{dt} \int_s \vec{B} \cdot d\vec{s} \quad (2.11) \quad \vec{\nabla} \times \vec{E} = -\frac{d\vec{B}}{dt} \quad (2.12)$$

Were, \vec{E} is the electric field.

\vec{B} is the magnetic field.

c is a given closed path.

$d\vec{L}$ is a small vector that is tangential to the path at every point.

s is the surface bounded by the path c.

In eq. (2.11), if c is the path followed by the wire of the Rogowski coil, and s is the area bound the coil, then; $\int_s \vec{B} \cdot d\vec{s} = \phi_T$ & $\oint_c \vec{E} \cdot d\vec{L} = \epsilon_V$. Using these equations, we have created a mathematical model, based on this equation to estimate the error due to the gap for the two types of coils shown in figure 2.11 and 2.12.

We make the following assumptions to simplify the integration of the magnetic field through the coil:

- The wire carrying current is of infinite length. i.e.; $\phi_1 = \phi_2 = 90^\circ$.
- The wire carrying current has negligible diameter.
- Every turn in the coil is assumed to be a closed loop.

We need:

$$error(\epsilon) = f(g, d, r, R, N)$$

Were, g is the gap in radians.

d is the displacement of the primary conductor towards the gap.

R is the outer radius of the coil.

r is the inner radius of the coil.

N is the number of turns in the coil.

We know that,

$$\epsilon = \frac{\mathcal{E}_{V(disp)} - \mathcal{E}_{V(centre)}}{\mathcal{E}_{V(centre)}}$$

From eq. (2.11), if the coil is in the centre:

$$\phi = \int_s \vec{B} \cdot \vec{ds} = \int_r^R \vec{B} \cdot \vec{ds} = \int_r^R \frac{\mu_0 i_p W}{2\pi x} dx = \frac{\mu_0 i_p W}{2\pi} \ln\left(\frac{R}{r}\right) \quad [2], \text{ w is the thickness of the coil.}$$

$$\therefore \phi_T = N\phi = N * \frac{\mu_0 i_p W}{2\pi} \ln\left(\frac{R}{r}\right)$$

$$\mathcal{E}_{V(centre)} = -\frac{d\phi_T}{dt} = -\frac{d}{dt}\left(N * \frac{\mu_0 i_p W}{2\pi} \ln\left(\frac{R}{r}\right)\right) = -N * \frac{\mu_0 W}{2\pi} \ln\left(\frac{R}{r}\right) \frac{di_p}{dt} \quad (2.13)$$

Comparing eq. (2.13) to eq. (2.10), coefficient of mutual inductance when the coil is in the centre is:

$$M = N * \frac{\mu_0 W}{2\pi} \ln\left(\frac{R}{r}\right)$$

Assuming i_p is an alternating current of amplitude A & frequency f;

$$i_p = A * \sin(2\pi ft)$$

Substituting the value of i_p in eq. (2.13) we get:

$$\mathcal{E}_{V(centre)} = -N * \frac{\mu_0 W}{2\pi} \ln\left(\frac{R}{r}\right) \frac{d}{dt}(A * \sin(2\pi ft)) = -NA2\pi f * \frac{\mu_0 W}{2\pi} \ln\left(\frac{R}{r}\right) \cos(2\pi ft).$$

If the conductor is not in the centre;

$$\mathcal{E}_{V(disp)} = \sum_{i=1}^N A2\pi f * \frac{\mu_0 W}{2\pi} \ln\left(\frac{R_i}{r_i}\right) \cos(2\pi ft) \quad (2.14)$$

Were, R_i & r_i are the perpendicular distance between the conductor and the inner and outer side of each loop.

$$\therefore R_i = \sqrt{\left(R * \cos\left(\frac{g}{2} + \frac{(2\pi-g)(i-1)}{N-1}\right) - d\right)^2 + \left(R \sin\left(\frac{g}{2} + \frac{(2\pi-g)(i-1)}{N-1}\right)\right)^2}$$

$$\& \quad r_i = \sqrt{\left(r * \cos\left(\frac{g}{2} + \frac{(2\pi-g)(i-1)}{N-1}\right) - d\right)^2 + \left(r \sin\left(\frac{g}{2} + \frac{(2\pi-g)(i-1)}{N-1}\right)\right)^2}$$

$$\therefore \epsilon = \frac{\left(\sum_{i=1}^N A2\pi f * \frac{\mu_0 W}{2\pi} \ln\left(\frac{R_i}{r_i}\right) \cos(2\pi ft)\right) - NA2\pi f * \frac{\mu_0 W}{2\pi} \ln\left(\frac{R}{r}\right) \cos(2\pi ft)}{NA2\pi f * \frac{\mu_0 W}{2\pi} \ln\left(\frac{R}{r}\right) \cos(2\pi ft)}$$

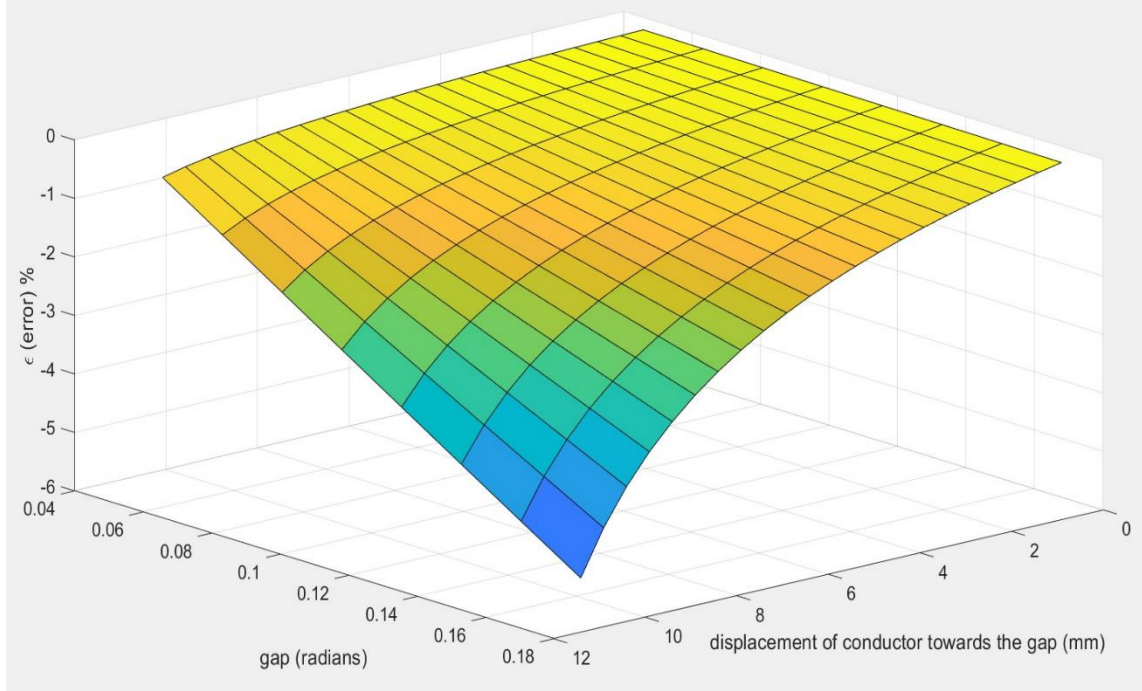
After simplification, we get:

$$\epsilon = \frac{\left(\sum_{i=1}^N \ln\left(\frac{R_i}{r_i}\right)\right) - \ln\left(\frac{R}{r}\right)}{\ln\left(\frac{R}{r}\right)} \quad \dots (2.15)$$

Substituting the value of R_i and r_i in eq. (2.15):

$$\therefore \epsilon = \frac{\left(\sum_{i=1}^N \ln \left(\frac{\sqrt{(R \cos(\frac{g}{2} + \frac{(2\pi-g)(i-1)}{N-1}) - d)^2 + (R \sin(\frac{g}{2} + \frac{(2\pi-g)(i-1)}{N-1}))^2}}{\sqrt{(r \cos(\frac{g}{2} + \frac{(2\pi-g)(i-1)}{N-1}) - d)^2 + (r \sin(\frac{g}{2} + \frac{(2\pi-g)(i-1)}{N-1}))^2}} \right) \right) - \ln \left(\frac{R}{r} \right)}{\ln \left(\frac{R}{r} \right)} \quad (2.16)$$

We have plotted eq. (2.16) for $R = 20\text{mm}$, $r = 13.25$, $d = [0.5, 11]$ and $N = 152$ and the gap $[3^0, 10^0]$ and got the following result.



Graph 2.11: Gap v/s Displacement v/s Error

From the graph it can be seen that error increases with increase in displacement and increase in gap.

Error due to magnetic field by a wire close to the coil:

Gap also makes to coil vulnerable to errors, due to the changing magnetic field of any wire carrying alternating current close to the outer diameter of the coil. This error is maximum when the wire is close to the gap. If the distance between the wire and the outer end of the coil is known, then we can estimate the voltage induced in the coil using eq. (2.14) as shown below.

$$\mathcal{E}_V = A2\pi f * \frac{\mu_0 W}{2\pi} \sum_{i=1}^N \ln \left(\frac{R_i}{r_i} \right) \cos(2\pi f t) \quad (2.14)$$

In this case, if d is the distance between the outer edge of the coil, then

$$R_i = \sqrt{\left(R * \cos \left(\frac{g}{2} + \frac{(2\pi-g)(i-1)}{N-1} \right) - (d + R) \right)^2 + \left(R \sin \left(\frac{g}{2} + \frac{(2\pi-g)(i-1)}{N-1} \right) \right)^2}$$

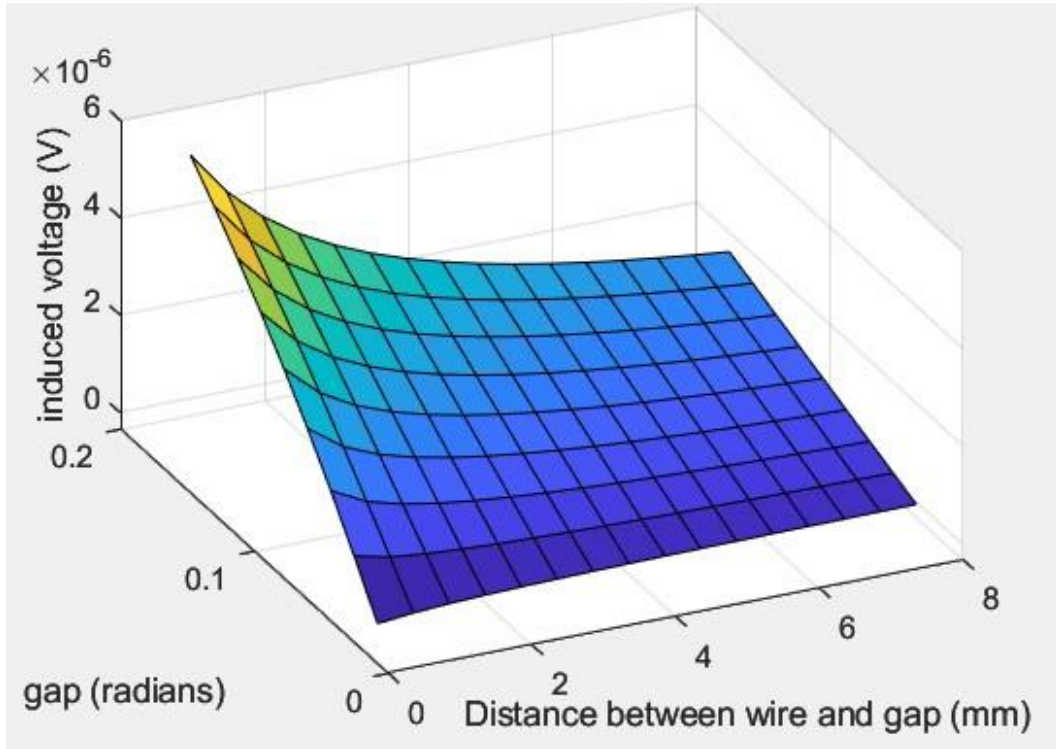
$$\& \quad r_i = \sqrt{\left(r * \cos \left(\frac{g}{2} + \frac{(2\pi-g)(i-1)}{N-1} \right) - (d + R) \right)^2 + \left(r \sin \left(\frac{g}{2} + \frac{(2\pi-g)(i-1)}{N-1} \right) \right)^2}$$

Substituting, R_i & r_i in eq. (2.14);

$$\mathcal{E}_V = A2\pi f *$$

$$\frac{\mu_0 W}{2\pi} \sum_{i=1}^N \ln \left(\frac{\sqrt{(R \cos(\frac{g}{2} + \frac{(2\pi-g)(i-1)}{N-1}) - (d+R))^2 + (R \sin(\frac{g}{2} + \frac{(2\pi-g)(i-1)}{N-1}))^2}}{\sqrt{(r \cos(\frac{g}{2} + \frac{(2\pi-g)(i-1)}{N-1}) - (d+R))^2 + (r \sin(\frac{g}{2} + \frac{(2\pi-g)(i-1)}{N-1}))^2}} \right) \cos(2\pi f t) \quad (2.17)$$

Plotting the above equation for $N = 152$, for $R = 20\text{mm}$, $r = 13.25$, $d = [0.5, 11]$ and $[3^0, 10^0]$ and got the following result.



Graph 2.12: Distance v/s Gap v/s Induced voltage

Note: the conductor is outside the sensor hole, distance is measured from outer diameter.

As expected, the graph shows that the induced voltage increases with increase in gap and reduces as the wire moves away from the coil. Eq. (2.16) and eq. (2.17) are derived with some simplifying assumptions. To check if these assumptions have any impact on the accuracy of our results, we will compare these results with a finite element model and results obtained by physical experiments.

2.2.2 By finite element modelling

Steps to create a finite element model are as follows:

1. Geometry creation on any C.A.D. software like Creo, Solidworks, Fusion 360 etc.
2. Specifying solution type.
3. Applying boundary conditions.

4. Creating solution setup and setting mesh parameters (discretization of the given problem).
5. solving the model for required results.

Geometry creation:

The complete geometry of the coils shown in figure 6 and 7 is actually reasonably complicated. We have created a simplified model of these coils with the same number of turns, and the same value of internal and external radius using Creo 9.0.0.0. The steps for creating this geometry in creo are explained below.

1. Create an arc of mean radius with a gap similar to the real coil shown below.

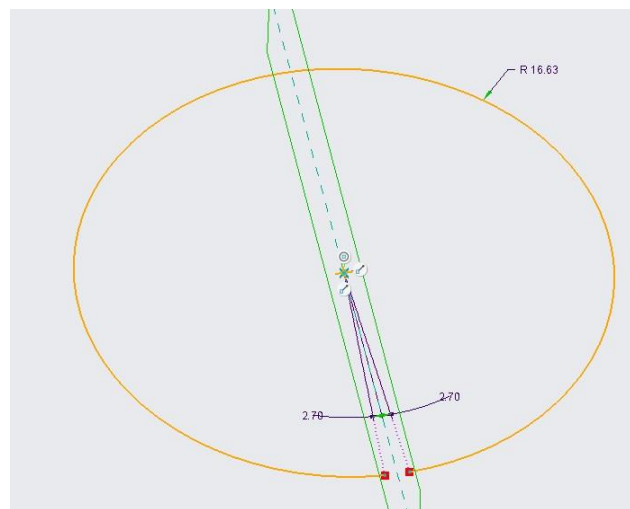


Figure 2.13: arc created with mean radius and given gap

The gap is approximated by importing a schematic of the coil into Creo as shown in the figure below.

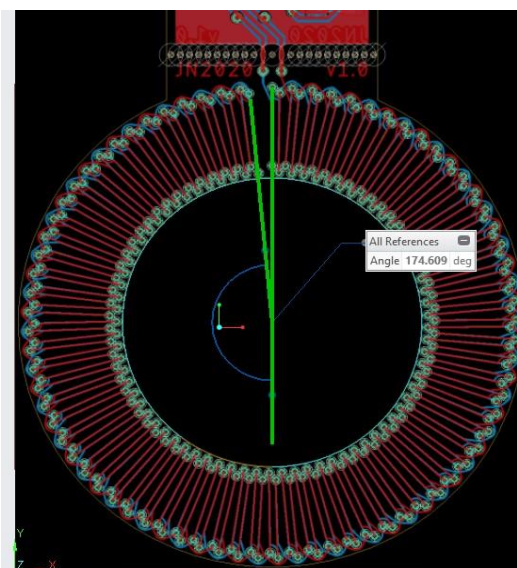


Figure 2.14: Measuring the gap ($\approx 5.4^0$)

2. Creating a hollow ring using surface sweep using the arc as path with the given inner and outer radius.

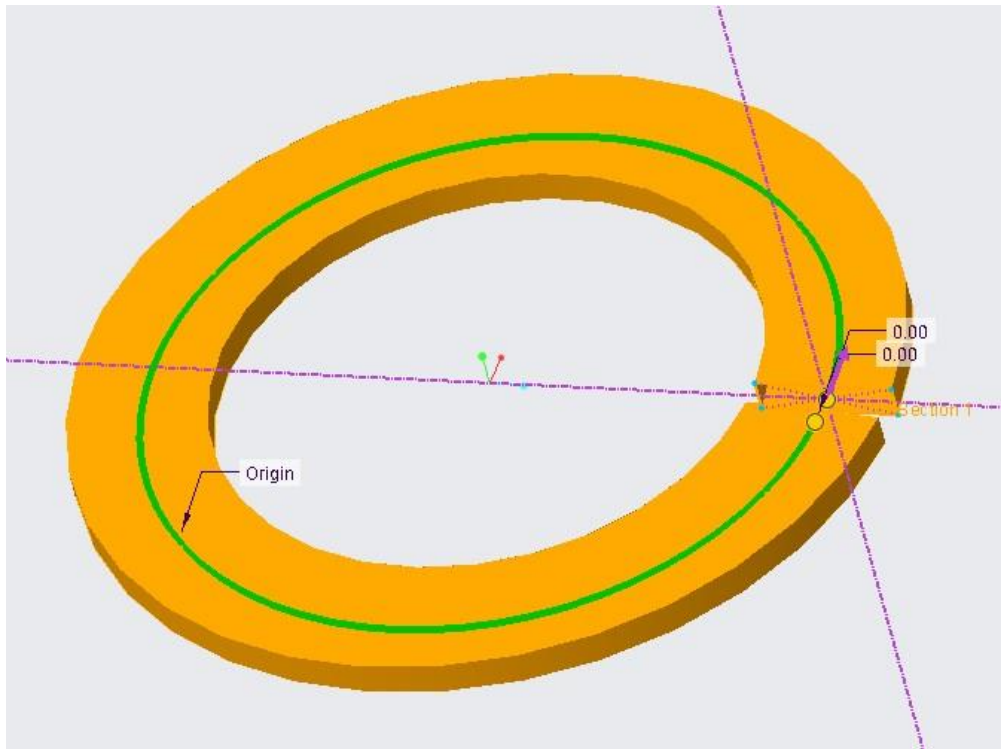


Figure 2.15: Ring created using sweep command

3. Create another surface that is wrapped helically around the ring.

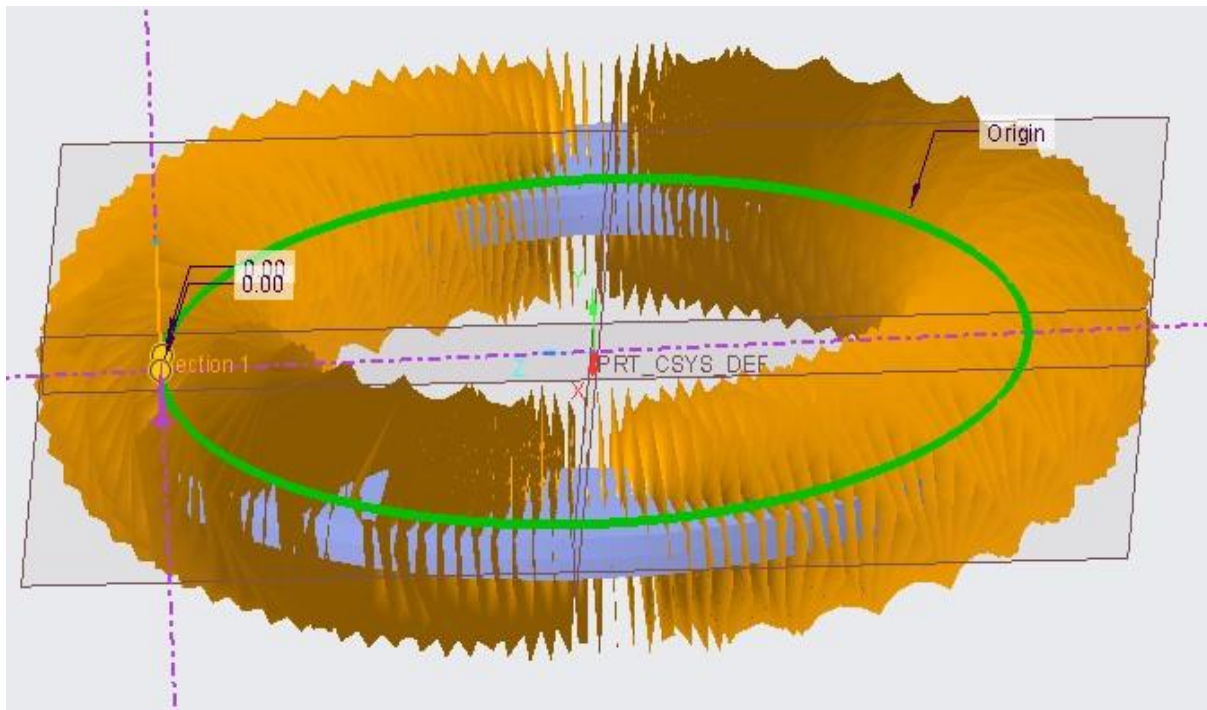


Figure 2.16: 2nd sweep

The 2nd sweep is created by establishing a relationship between the dimensions of the sketch and TRAJPAR parameter.

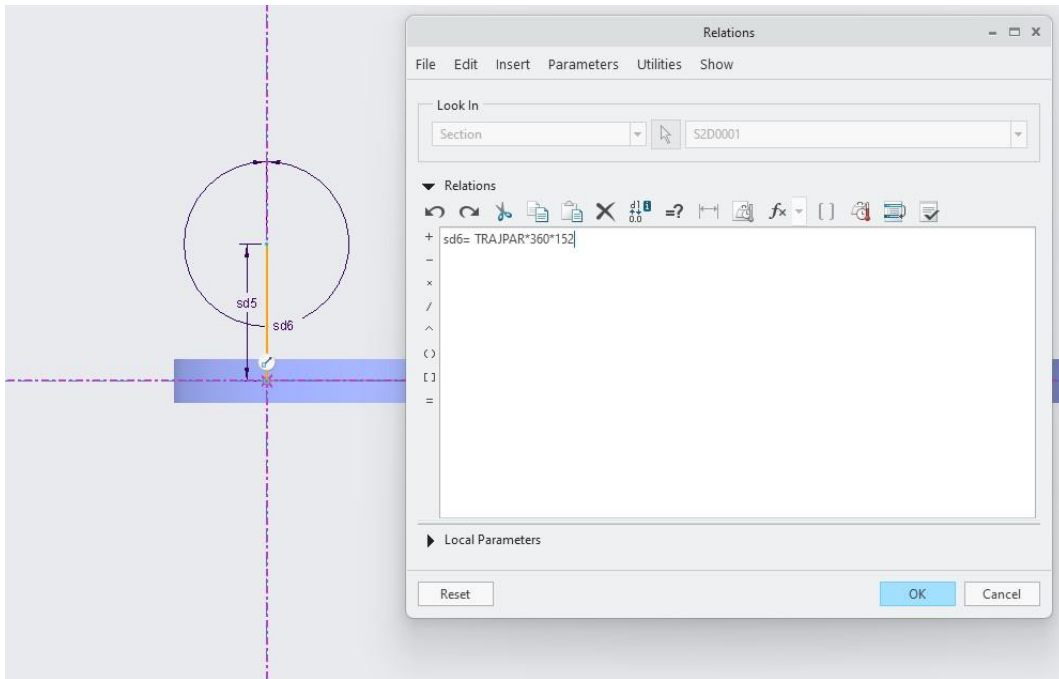


Figure 2.17: Relationship between sd6 and sweep

The TRAJPAR parameter goes from 0 to 1 through the given sweep path. Sd6 is the angle of the line with the vertical. Applying the relation as shown in the figure, we can ensure that the 2nd surface makes 152 turns around the ring.

4. Finding the intersection between the surfaces using intersect command.

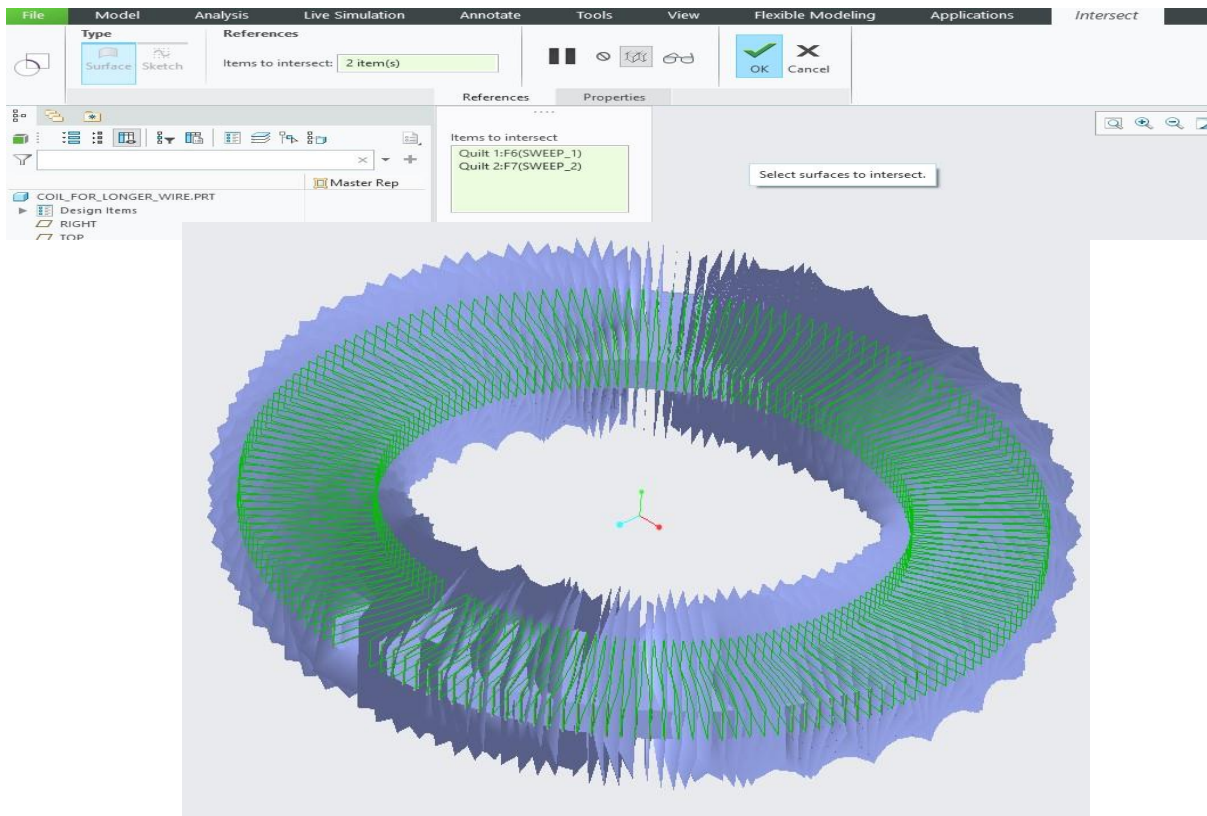


Figure 2.18: Intersection between the swept surfaces

5. Sweeping across the given path of intersection.

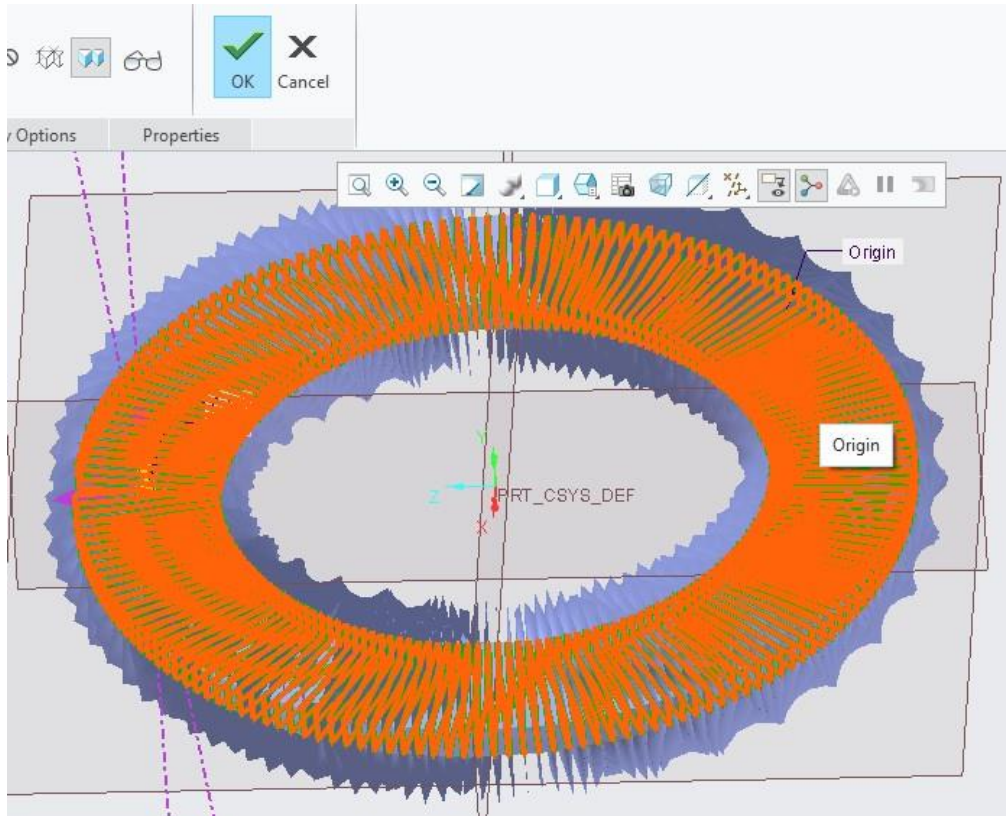


Figure 2.19: Sweep along the intersection

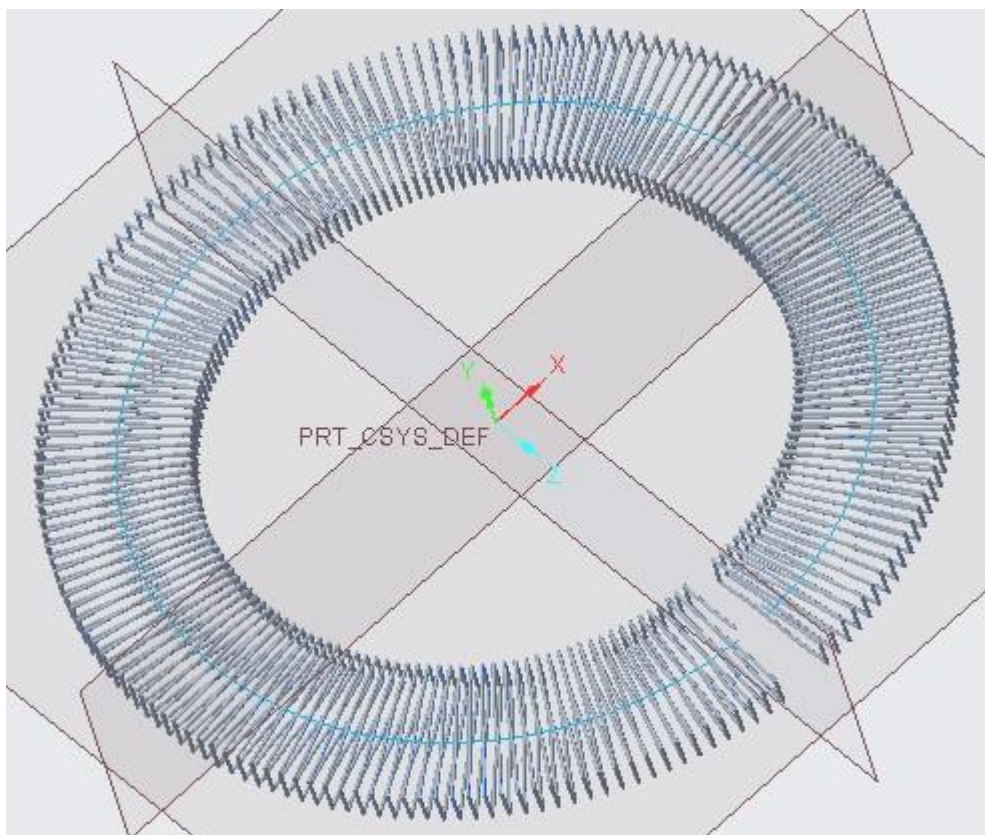


Figure 2.20: Coil without reference surfaces

The coil was swept with a hexagonal cross-section to improve to reduce the computational time of the analysis.

6. Creating coil terminals.

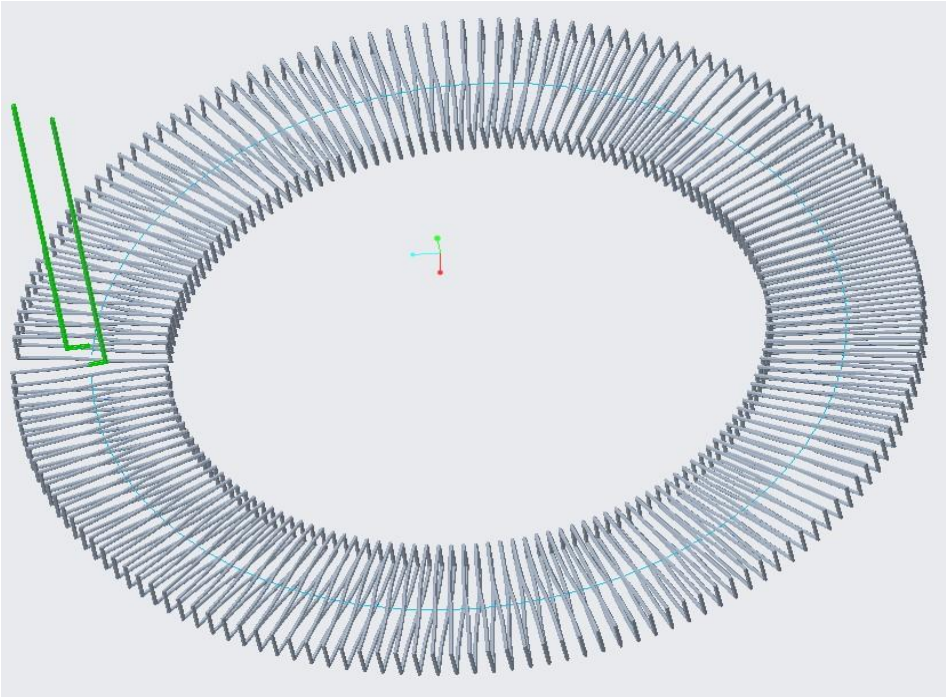


Figure 2.21: Coil terminals

These terminals are required for setting up boundary conditions.

7. Exporting to model to fusion 360.

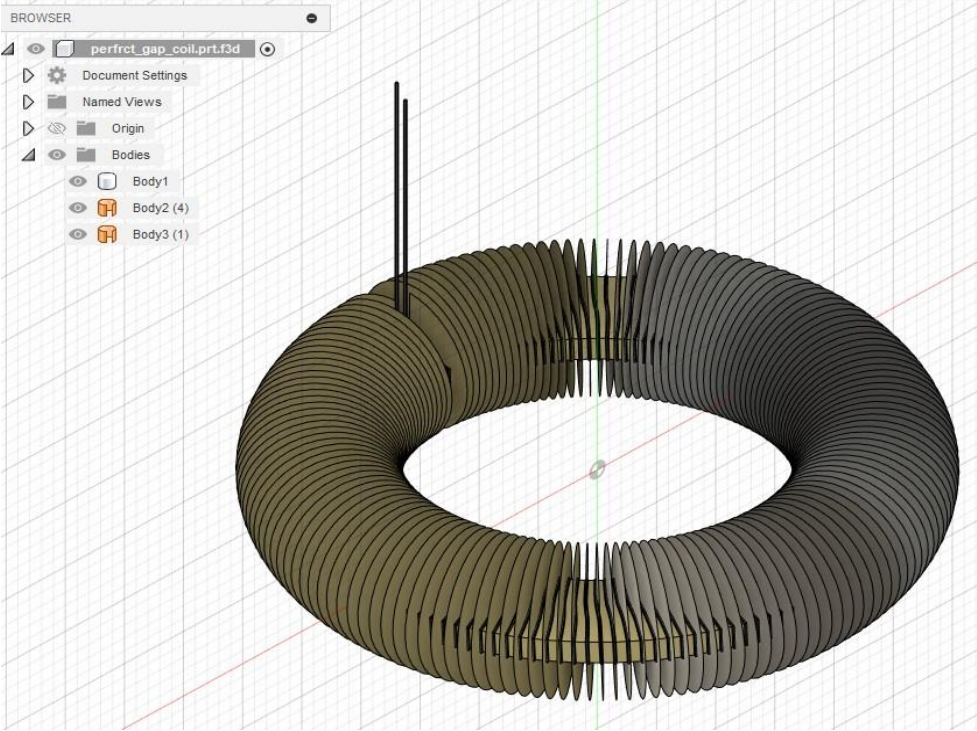


Figure 2.22: Coil in fusion 360

We import the coil to fusion 360 for 2 reasons:

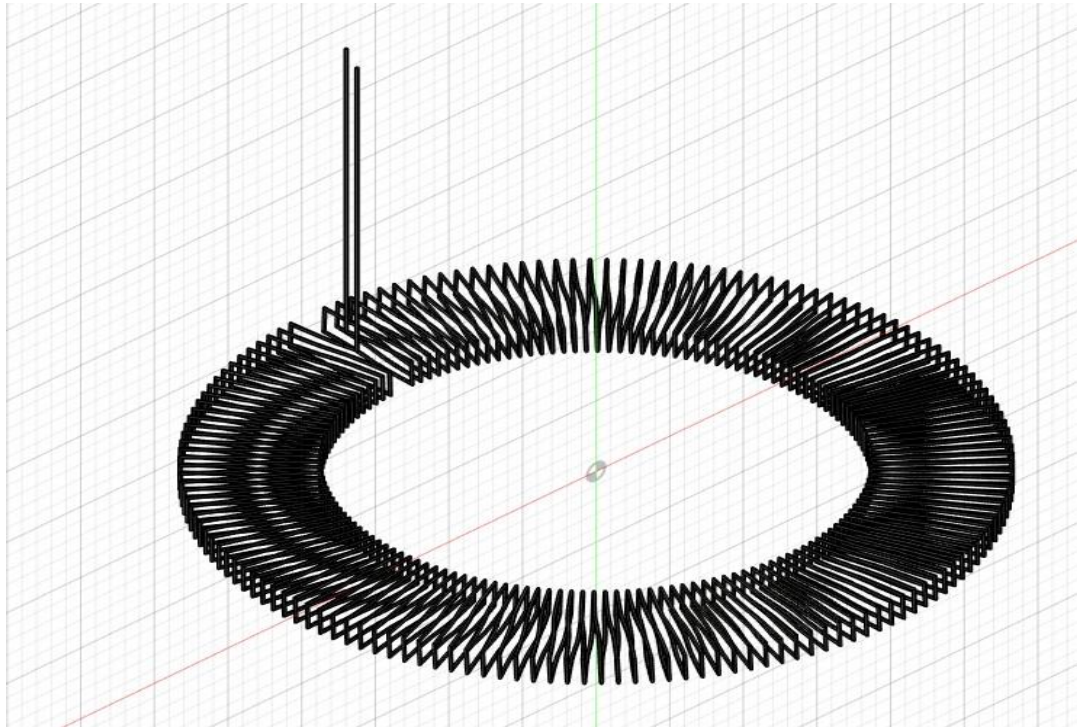


Figure 2.23: Final coil

- It is easy to delete the reference surfaces created in steps 2 and 3. We can simply select the surface body and delete it.
 - We can save the file in “. step” format which can be imported to Ansys maxwell for assigning the boundary conditions and solving the model.
8. The coil is imported to Ansys Maxwell, and the current carrying conductor is first placed in the centre of the coil. The conductor is created using the “draw cylinder” command with a radius of 1mm.

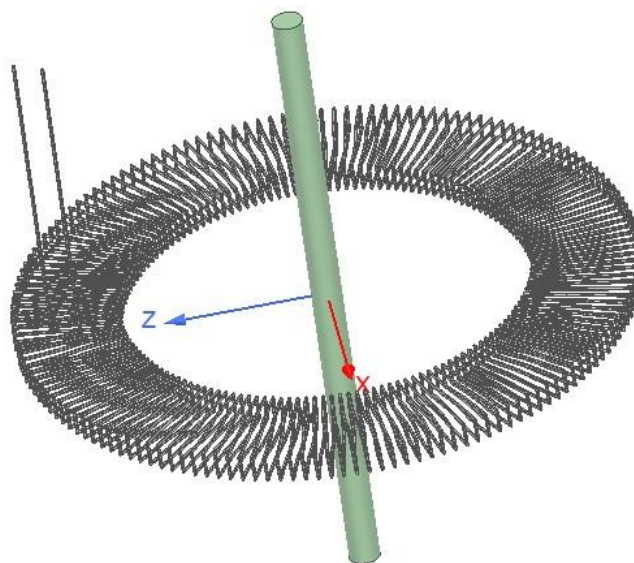


Figure 2.24: Coil with the conductor in centre

The following steps were followed to import the coil click on:

Maxwell 3D ⇒ modeller ⇒ import ⇒ select the coil ⇒ open.

The image below, shows the main part of the Ansys Maxwell G.U.I. it is useful for explaining the further steps in the analysis.

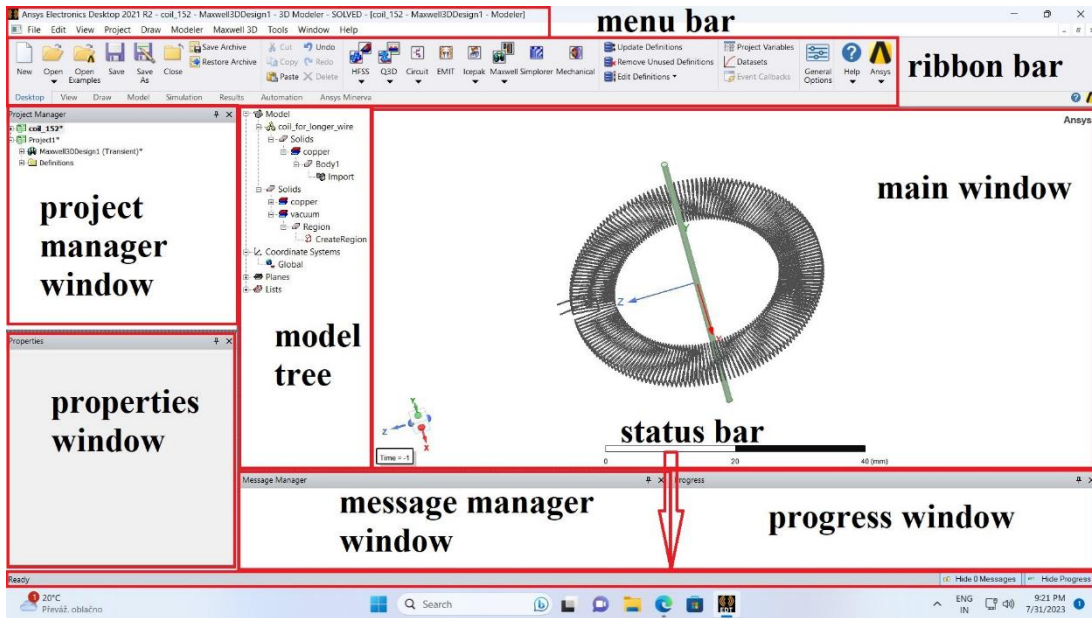


Figure 2.25: Ansys Maxwell G.U.I.

Specifying solution type:

Our problem is a magnetic transient problem. To setup the solution type click on:

Maxwell 3D (from the menu bar at the top of the screen)



Solution type ⇒ magnetic ⇒ transient

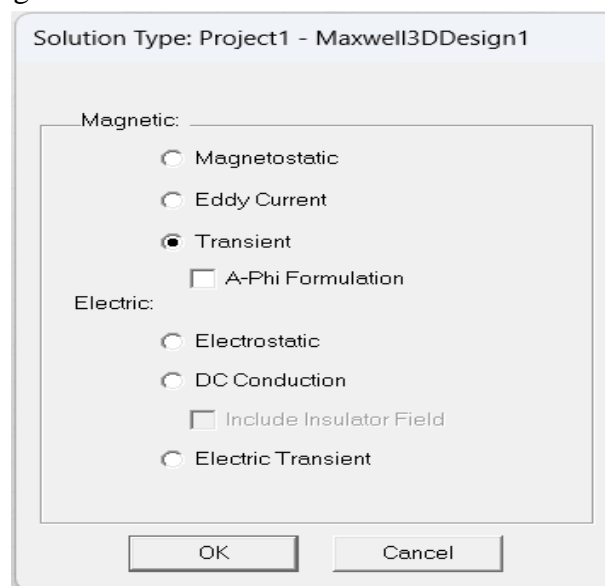


Figure 2.26: Specifying solution type

Applying boundary conditions:

- (i) Assign a material for the coil and the conductor. To do this right click on the imported body in the model tree and click on 'assign material'. A material selection window will appear as shown below. Select copper and click 'ok'.

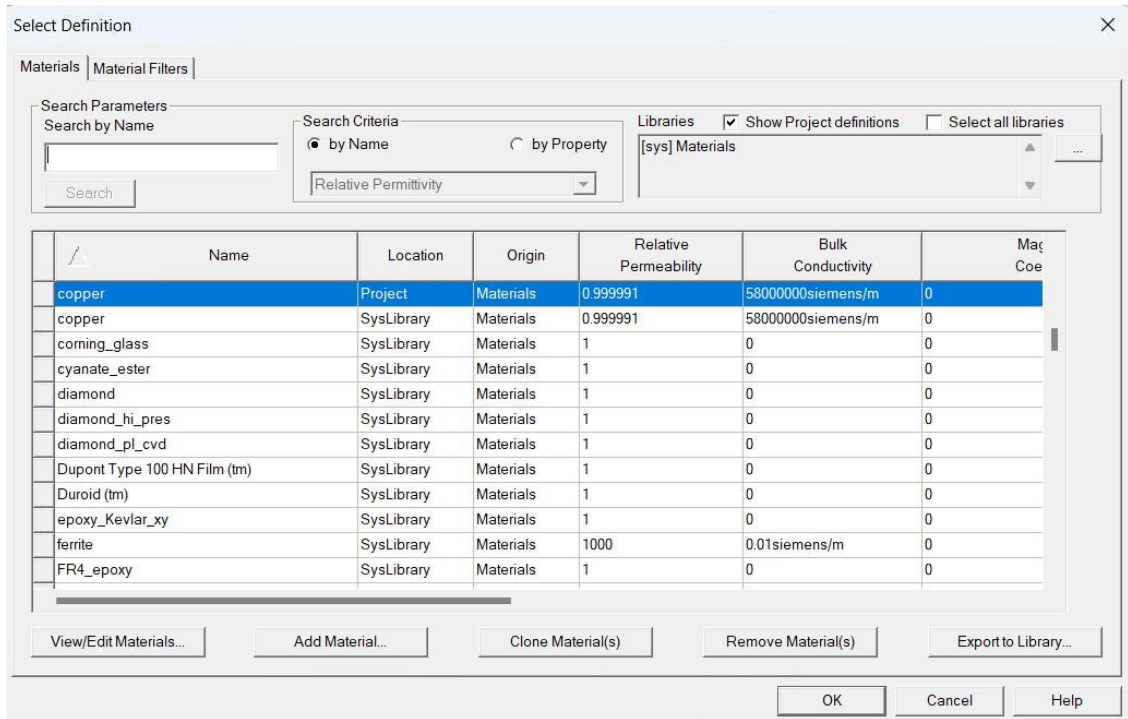


Figure 2.27: Material selection window

- (ii) Creating region of analysis. Click on create region command in draw tab of the ribbon bar.

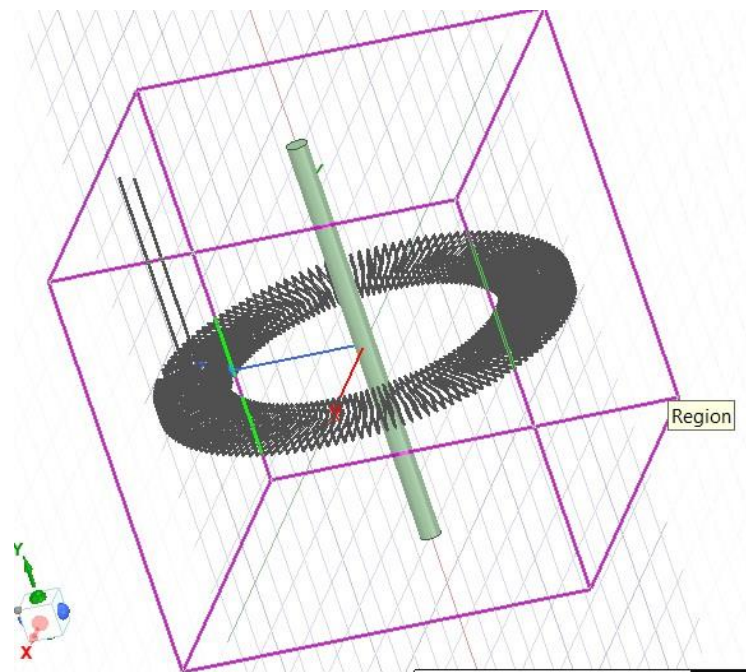


Figure 2.28: Region of analysis

(iii) To apply A.C. current through the conductor and calculate the induced alternating voltage, we need to define the conductor and coil as windings in Ansys Maxwell. To do this: expand the project in the project manager window ⇒ right click on excitations ⇒ add winding.

1. double click on the added winding, a new will open as shown in the figure.

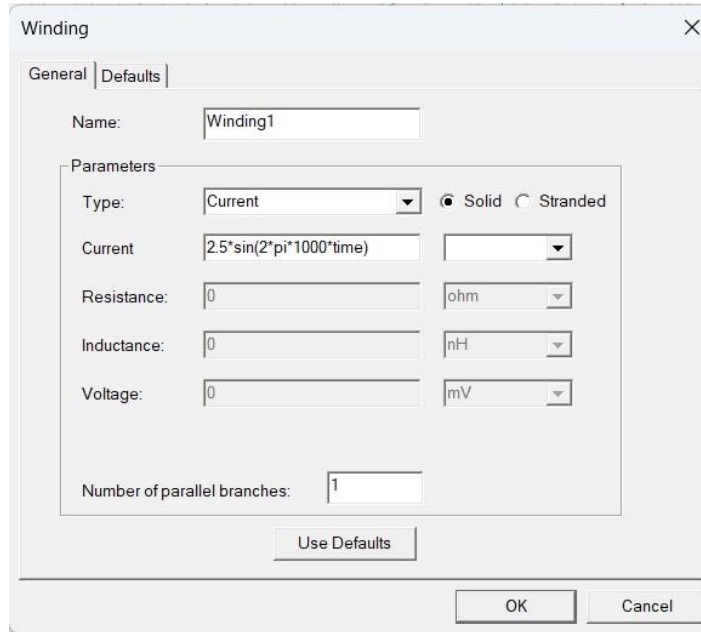


Figure 2.29: Applying current to the first winding

2. Similarly, create another winding for the coil, change the type to voltage and click ‘ok’.
- (iv) Assign coil terminals: select the face at the beginning of the conductor ⇒ right click on “Winding1” ⇒ assign coil terminals.
3. a new dialog box appears as shown in the figure.

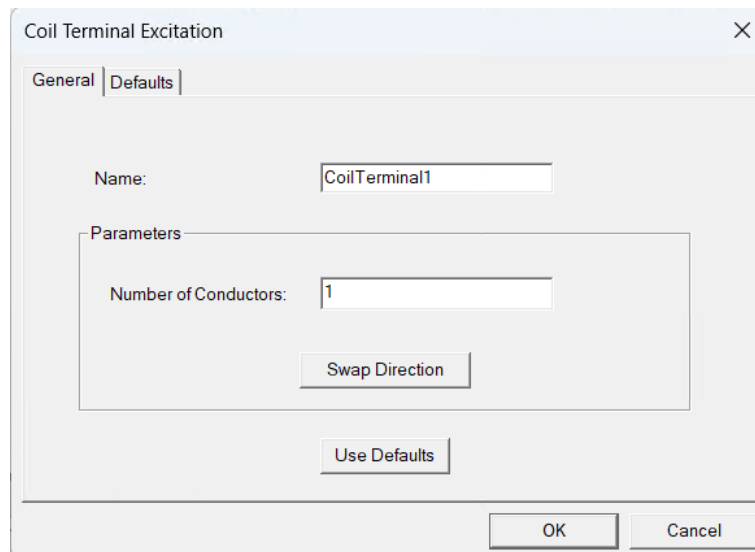


Figure 2.30: Coil terminal

- Set the “numbers of conductors” = 1, set the direction of coil terminal and click ‘ok’. This process should be repeated for the ends of the primary conductor and the ends of the coil. The direction of all four coil terminals is shown in the figures below.

Creating solution setup and setting mesh parameters:

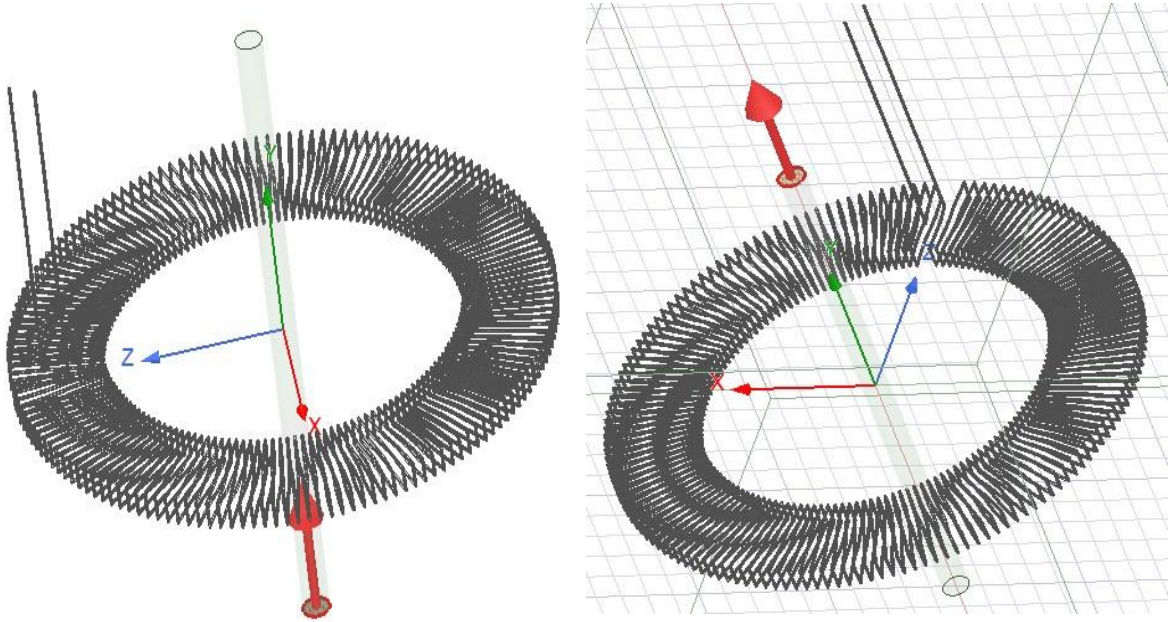


Figure 2.31: Direction of coil terminals for primary conductor

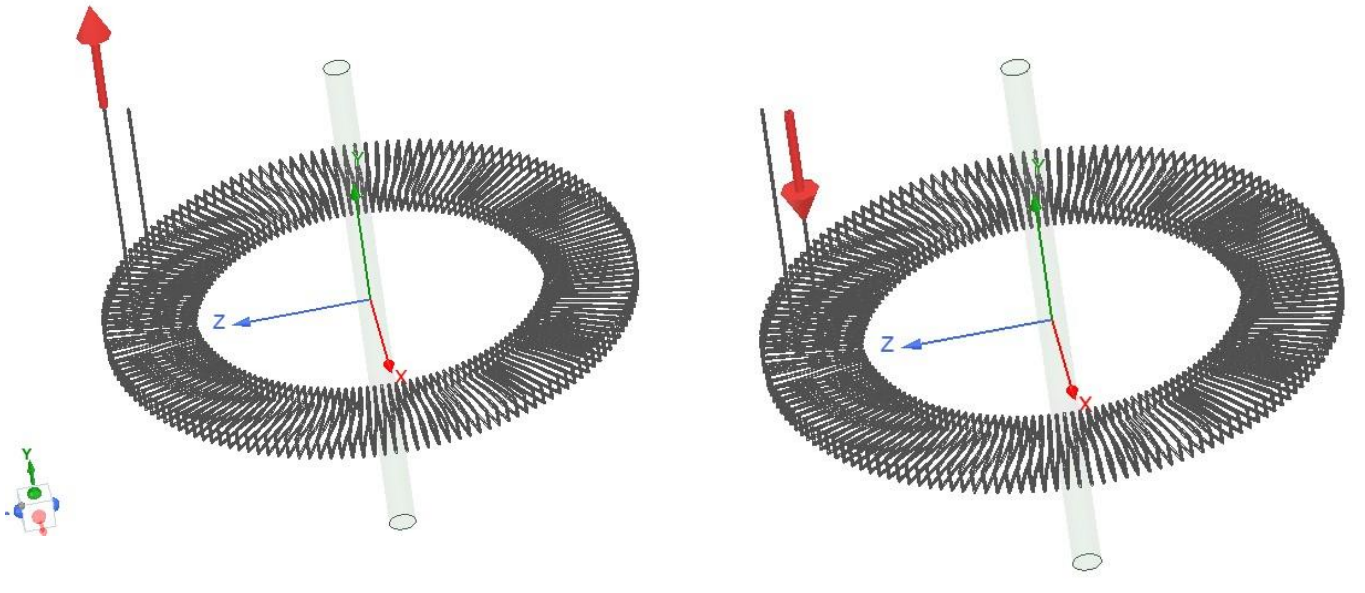


Figure 2.32: Direction of coil terminals for Rogowski coil

To approximate the geometry with reasonable accuracy we apply the surface approximation and surface priority as mesh parameters to the coil.

To apply these parameters, follow the steps as shown below:

select the coil from the model tree ⇒ right click on “body1” ⇒ assign mesh operation ⇒ surface approximation/surface priority for TAU.

A new dialog box will open as shown in the figure below

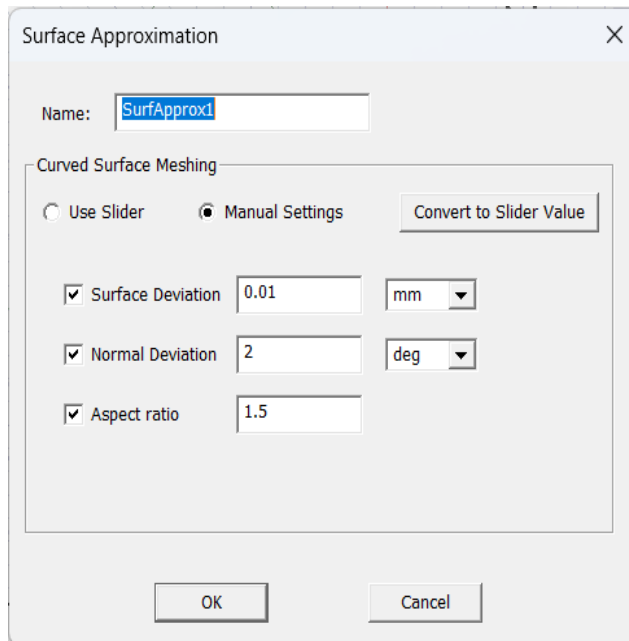


Figure 2.23: Setting surface approximation

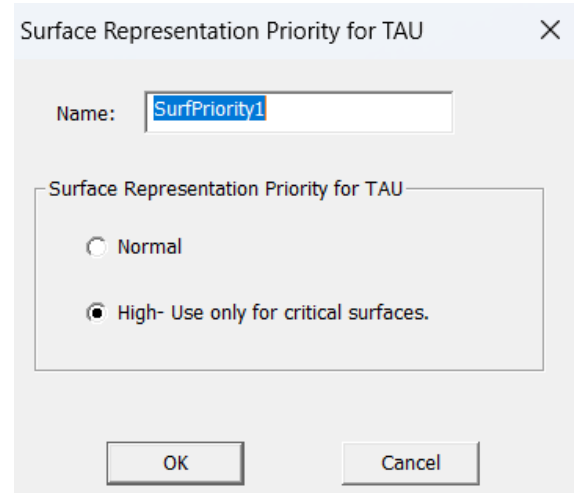


Figure 2.34: selecting surface for TAU meshing

To create solution setup: right click on “analysis” in the project manager window ⇒ add solution setup. The following dialog box will open:

In our case, we have an alternating with an amplitude of 2.5 A and frequency of 1kHz. To get

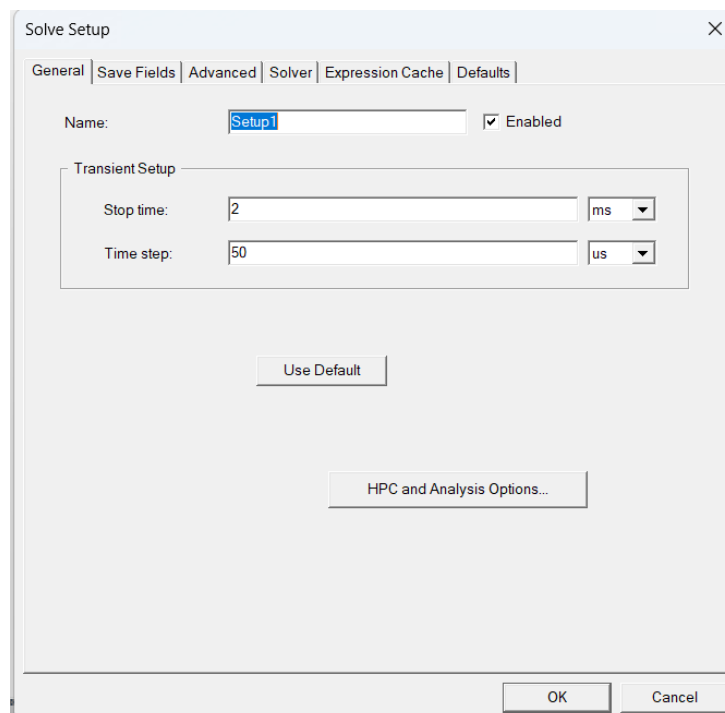


Figure 2.35: Solution setup

results for 2 periods, we need to analyse the model for 2 ms and we calculate the induced voltage

in the coil with a time step of 50 us. After setting these parameters, move to “save fields” tab and add parameters as shown in the figure below.

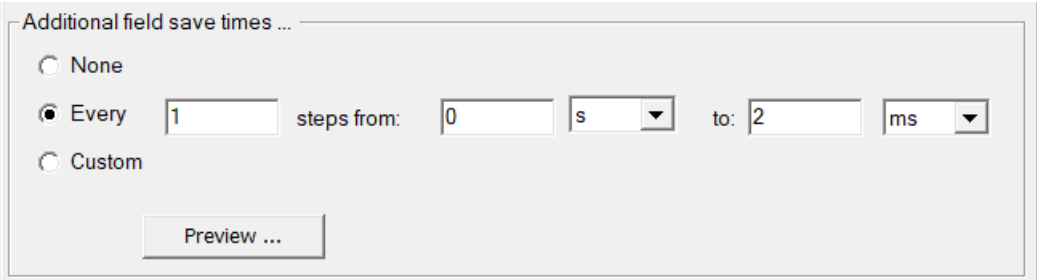


Figure 2.36: Saving the solution at every time step

This ensures that the solution calculated at the end of every time step is saved.

solving the model for required results:

To find the voltage induced in the coil at every time step; right click on “results” in the project manager window ⇒ create transient report ⇒ rectangular plot.

a new dialog box will open as shown in the figure below.

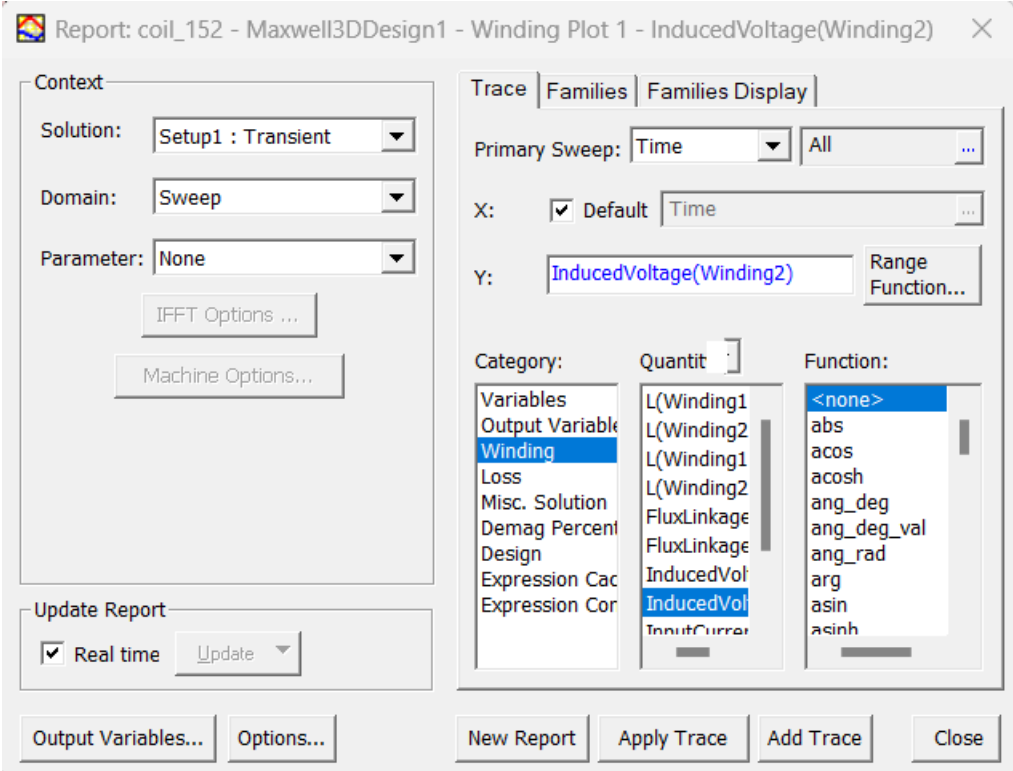
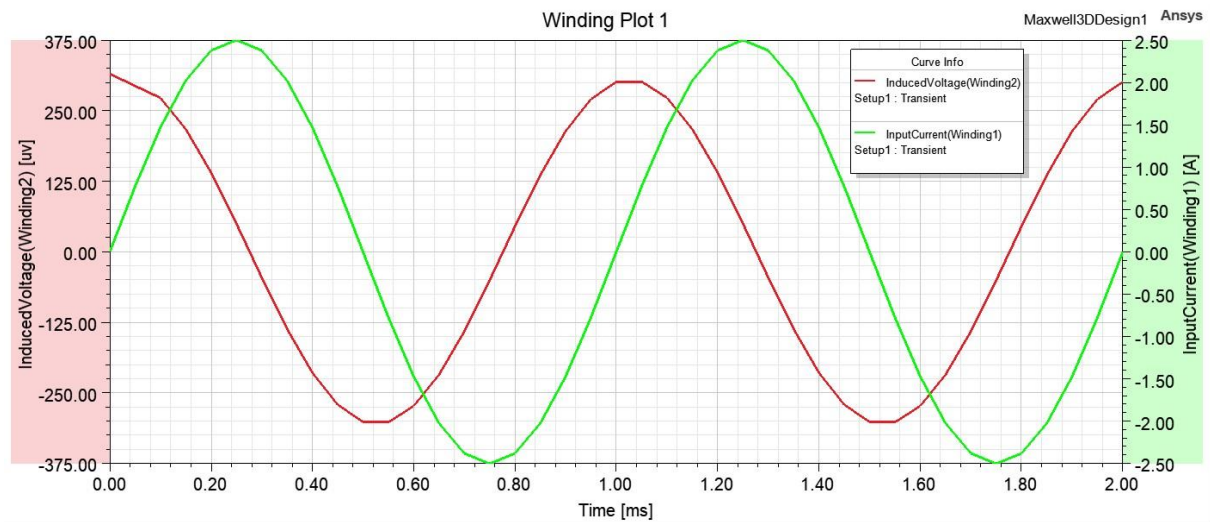


Figure 2.37: Specifying the required result

Select category: winding, quantity: induced voltage (winding 2), function: none. Click on apply trace. Similarly, we also select input current (winding 1) to see how the induced voltage varies with current. Right click on the project and click “analyse all”. The voltage induced in the coil and the current flowing through the conductor at every time step is shown in the graph below:



Graph 2.13: Induced voltage when the primary conductor is in the centre as seen from the graph:

the maximum induced voltage = 301.58 uV. & $V_{rms} = 218.34$ uV.

Now we run the same simulation again after moving the primary conductor near the gap (11 mm away from the the centre) as shown in the figure below.

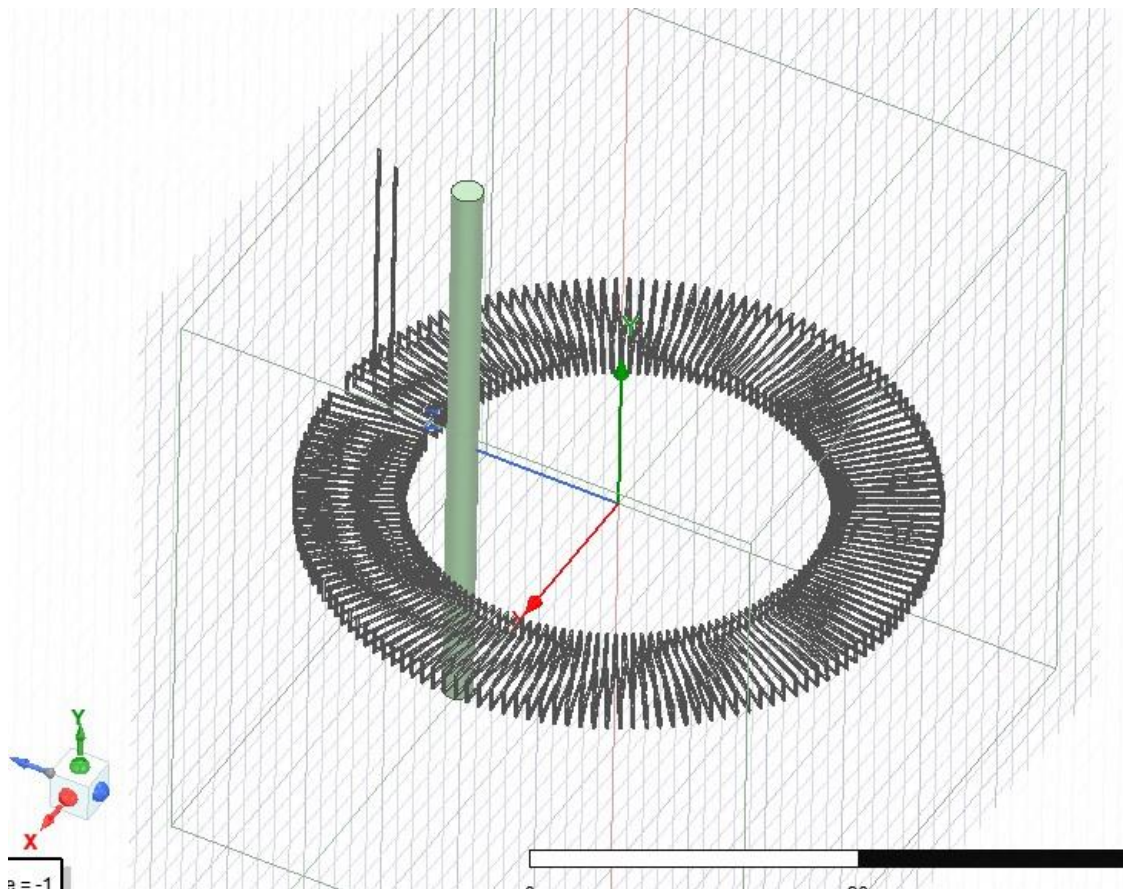
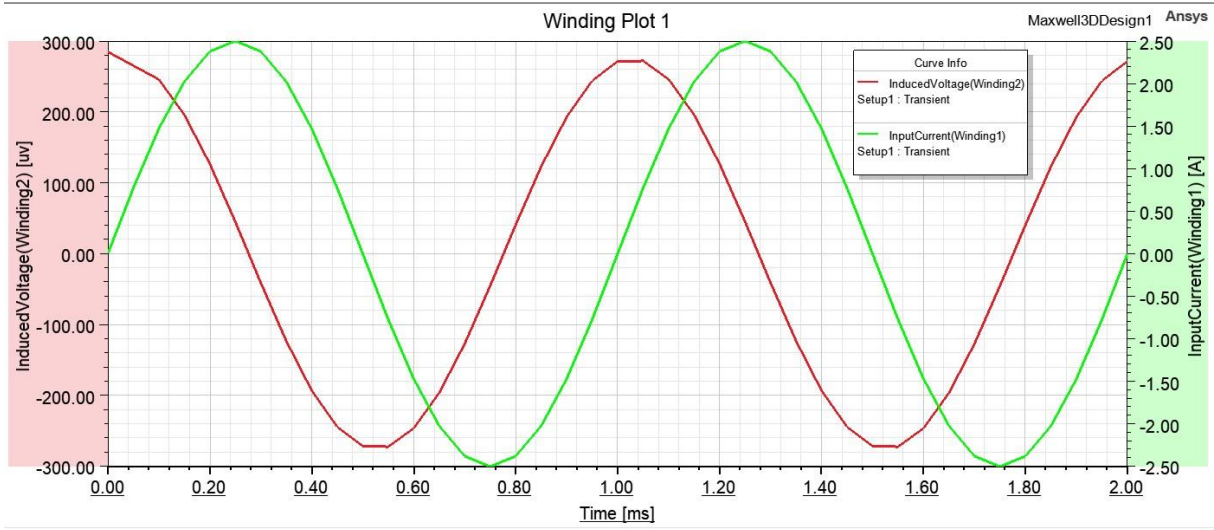


Figure 2.38: Primary conductor moved near the gap

The result of this simulation is shown in the graph below.



Graph 2.14: Induced voltage when the primary conductor is near the gap

As seen from the graph

the maximum induced voltage = 271.96 uV. & $V_{rms} = 196.93$ uV.

$$\text{therefore error} = \frac{271.96 - 301.58}{301.58} = 9.8\%$$

substituting the values of $\text{gap} = 5.4^0 * \pi / 180 \approx 0.0942$ and $R = 20$ mm, $r = 13.25$ mm, $d = 11$ mm and $N = 152$ in analytical formula we get:

$$\epsilon = \frac{\left(\sum_{i=1}^N \ln \left(\frac{\sqrt{\left(20 * \cos\left(\frac{0.0942}{2} + \frac{(2\pi - 0.0942)(i-1)}{152-1} \right) - 11 \right)^2 + \left(13.25 * \sin\left(\frac{0.0942}{2} + \frac{(2\pi - 0.0942)(i-1)}{152-1} \right) \right)^2}}{\sqrt{\left(13.25 * \cos\left(\frac{0.0942}{2} + \frac{(2\pi - 0.0942)(i-1)}{152-1} \right) - 11 \right)^2 + \left(13.25 * \sin\left(\frac{0.0942}{2} + \frac{(2\pi - 0.0942)(i-1)}{152-1} \right) \right)^2}} \right) - \ln\left(\frac{20}{13.25}\right)}{\ln\left(\frac{20}{13.25}\right)} \right) *$$

$$100 = -2.02\%$$

And peak induced voltage based on eq. (2.17) is:

$$\epsilon_V = 2.5 * 2\pi * 1000 *$$

$$\frac{\mu_0 W}{2\pi} \sum_{i=1}^N \ln \left(\frac{\sqrt{\left(20 * \cos\left(\frac{0.0942}{2} + \frac{(2\pi - 0.0942)(i-1)}{152-1} \right) - 11 \right)^2 + \left(20 * \sin\left(\frac{0.0942}{2} + \frac{(2\pi - 0.0942)(i-1)}{152-1} \right) \right)^2}}{\sqrt{\left(13.25 * \cos\left(\frac{0.0942}{2} + \frac{(2\pi - 0.0942)(i-1)}{152-1} \right) - 11 \right)^2 + \left(13.25 * \sin\left(\frac{0.0942}{2} + \frac{(2\pi - 0.0942)(i-1)}{152-1} \right) \right)^2}} \right) *$$

$$1 = 308.22 \text{ uV}$$

As we can see from the above results, the error calculated in the finite element model is much higher than the error calculated by the analytical formula. The reasons behind this difference are discussed in section 4 of this thesis.

2.2.3 Experimental measurement of error

Requirements:

- Siglent SDG1032X – Generator (for generating A.C. signal)
- Amplifier.
- C.N.C. bench for positioning of the primary conductor.
- N.I. measuring card. (For analog to digital conversion)

Method:

The basic setup of our experiment can be explained using the figure below.

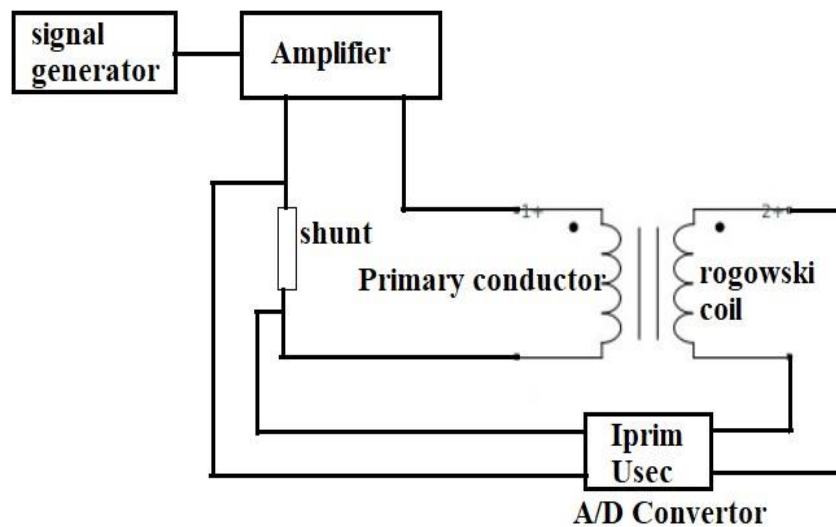


Figure 2.39: Schematic diagram of experiment

The signal generator is used to create a signal of 1 kHz and it is amplified to an amplitude to 2.5 A by the amplifier. This current is passed through the primary conductor and the voltage induced in the coil are measured and recorded using the measuring card. The sampling frequency of the A/D converter i.e.; the measuring card is set to 50 kHz to avoid problems related to aliasing [13]. This process is repeated for different positions of the primary conductor. The primary conductor and the coil are mounted the C.N.C. bench as shown in the figure below.

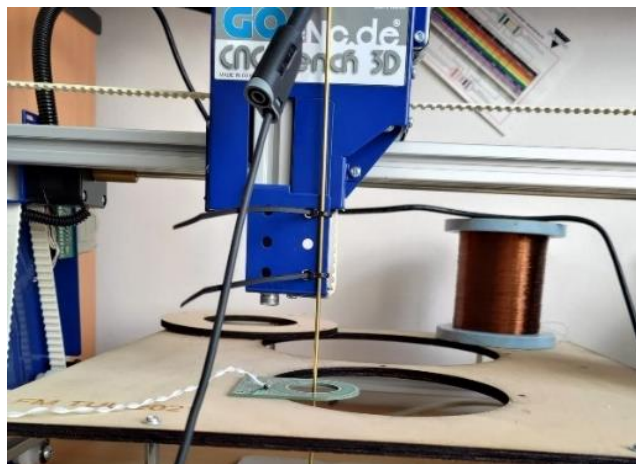


Figure 2.40: C.N.C. bench used for positioning the conductor

The C.N.C. bench is programmed to move the conductor to different positions before the start of every measurement. The complete setup of our experiment is shown in the figure below.

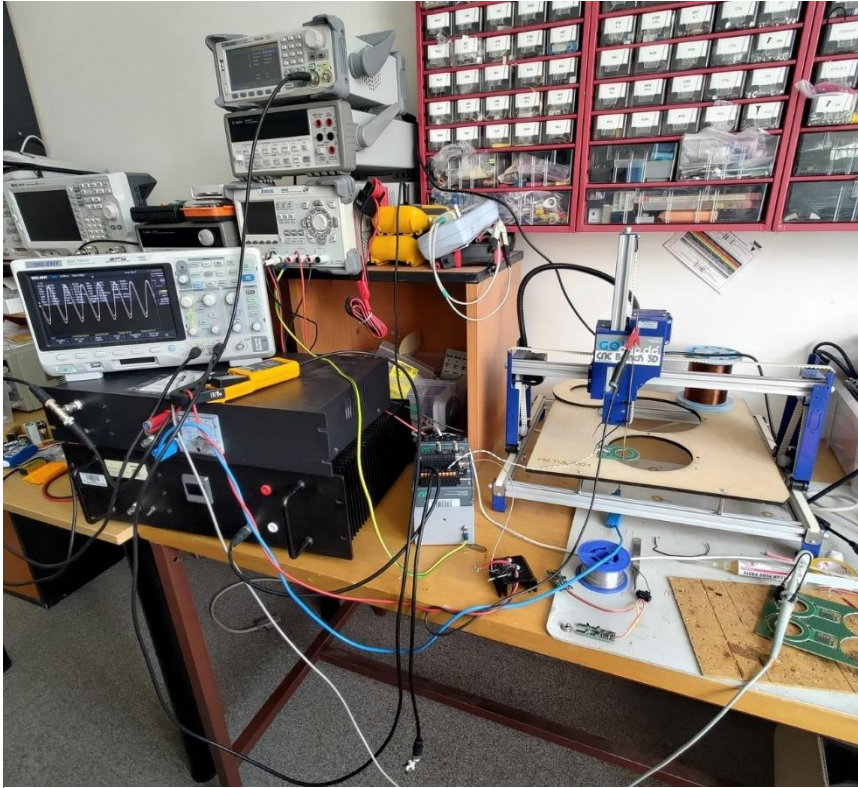
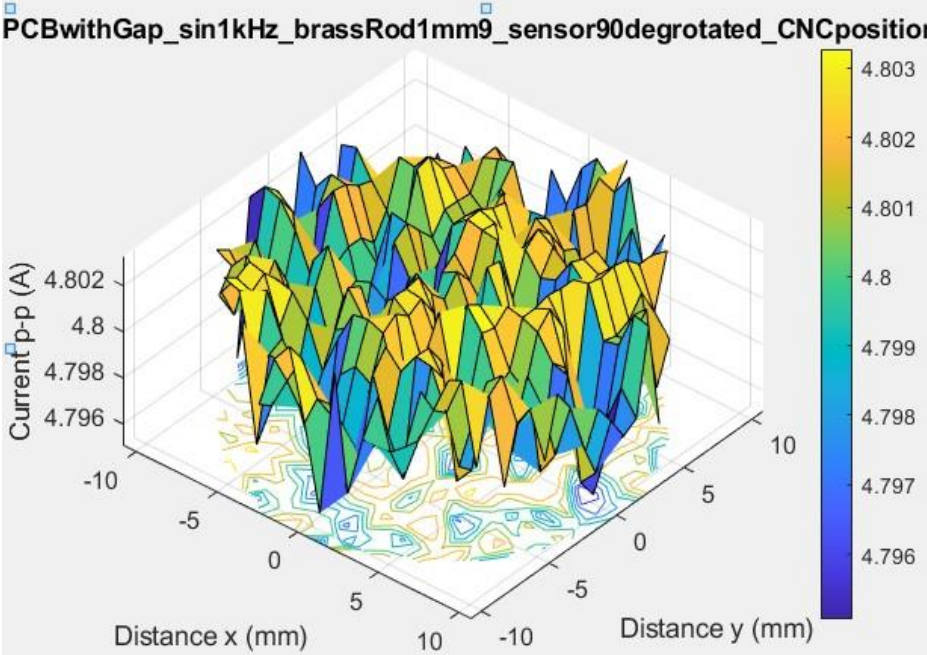


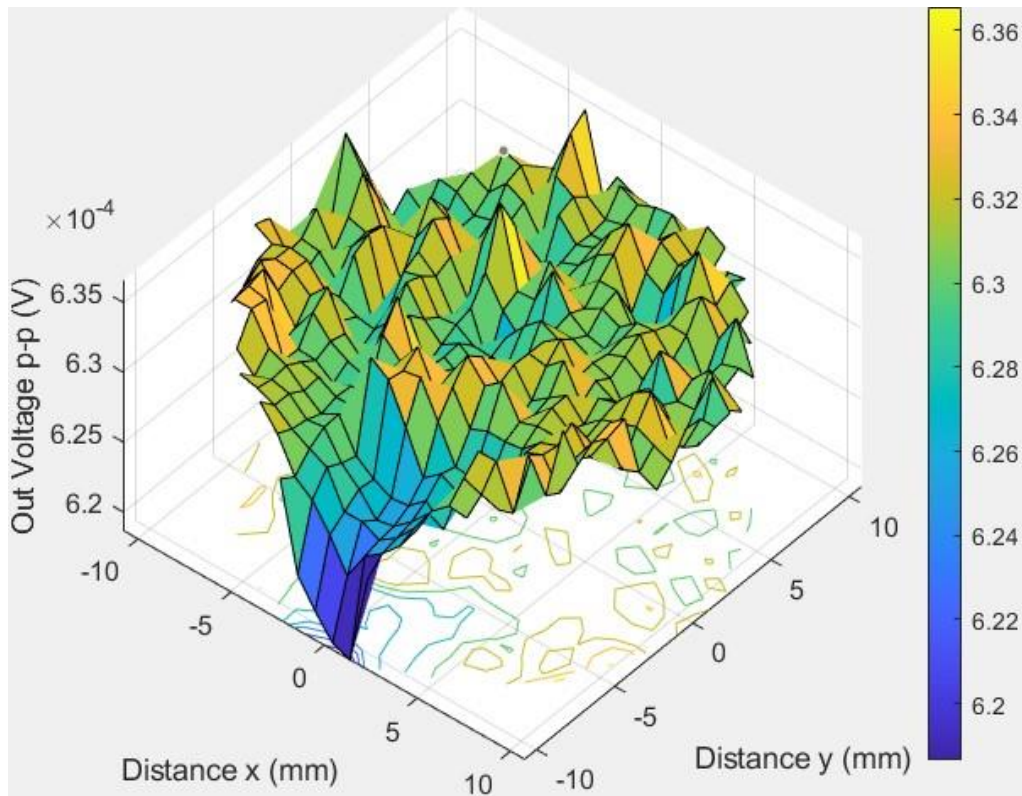
Figure 2.41: Complete setup of the experiment

Results:

The primary current and induced voltage measured at different points are shown in the graphs below.

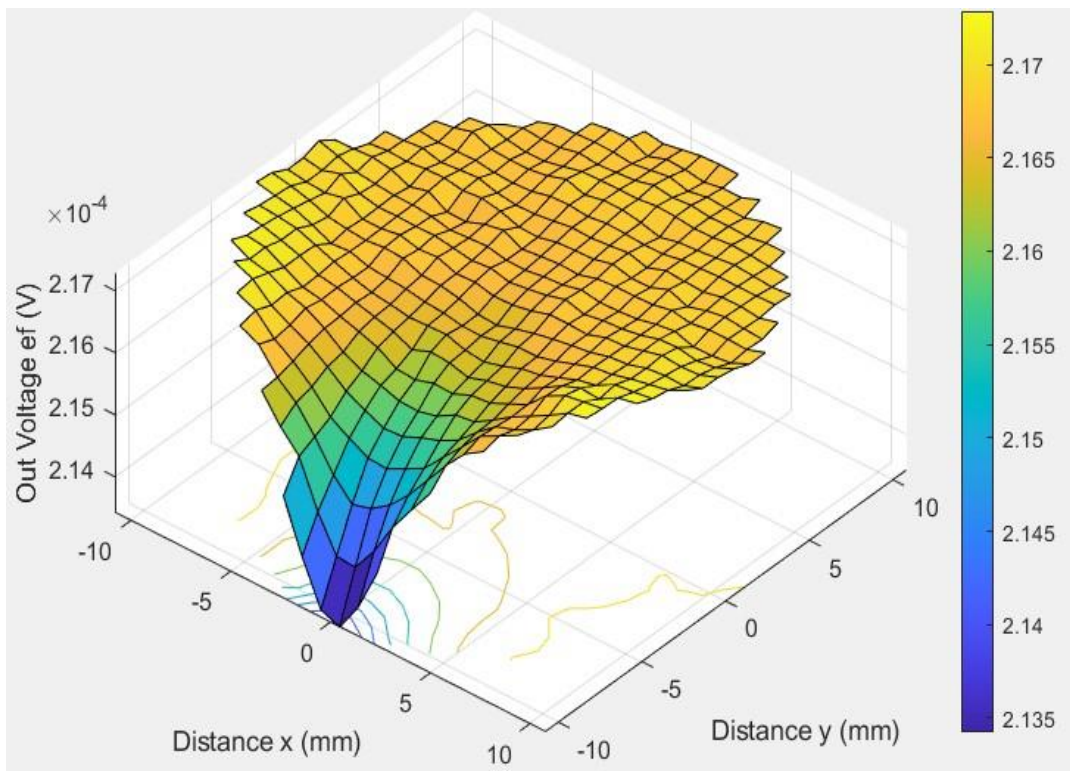


Graph 2.15: Primary Current (peak to peak)



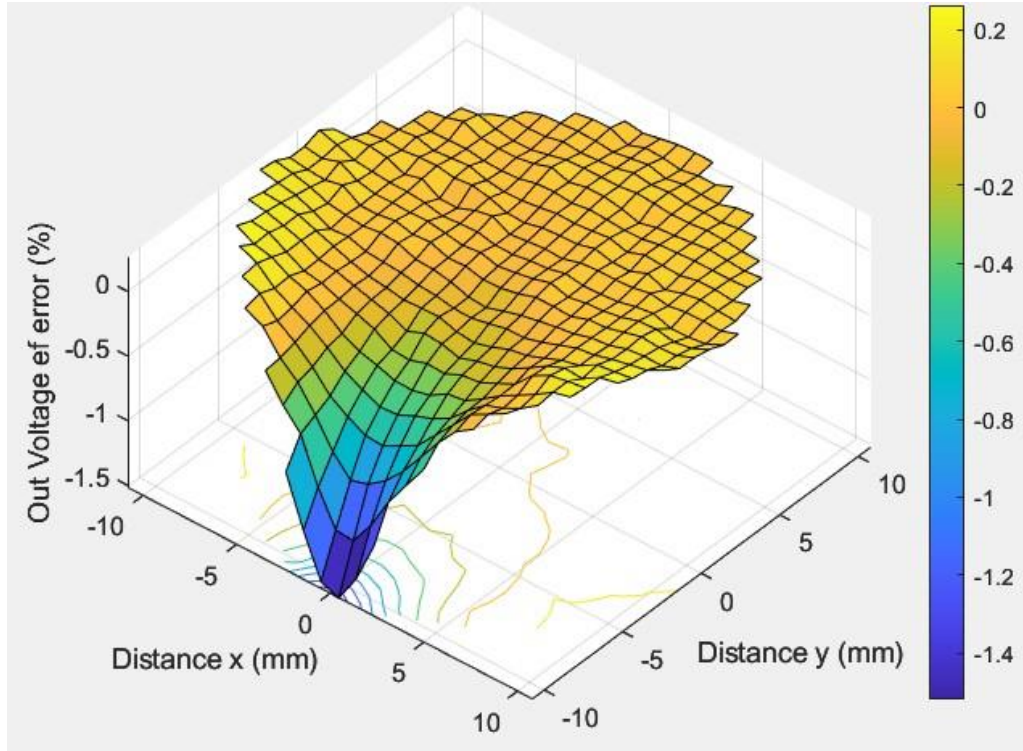
Graph 2.13: Induced voltage (peak to peak)

As we can see from the above graphs both measurements are affected by noise. To filter out this noise we calculate V_{RMS} (root mean square induced voltage) and then calculate the error at every point. The graphs show the calculated V_{RMS} at every point is shown below.



Graph 2.17: V_{RMS} of induced voltage

The error calculated at every point based on V_{RMS} voltage values are shown below.



Graph 2.18: Error induced due to gap

The maximum error induced to the gap is found to be about 1.51%.

2.3 Error approximation of split core Rogowski coil

2.3.1 With the help of analytical formulae

To calculate the total induced voltage, we will calculate the voltage induced in each half as shown below. (Assumptions are same as considered in section 2.2.1)

$$\mathcal{E}_{V1} = A2\pi f * \frac{\mu_0 W}{2\pi} \sum_{i=1}^{\frac{N}{2}} \ln \left(\frac{\sqrt{\left(R * \cos\left(\frac{(\pi)(i-1)}{\left(\frac{N}{2}\right)-1} \right) - d \right)^2 + \left(R \sin\left(\frac{(\pi)(i-1)}{\left(\frac{N}{2}\right)-1} \right) + g/2 \right)^2}}{\sqrt{\left(r * \cos\left(\frac{(2\pi-g)(i-1)}{\left(\frac{N}{2}\right)-1} \right) - d \right)^2 + \left(r \sin\left(\frac{(\pi)(i-1)}{\left(\frac{N}{2}\right)-1} \right) + g/2 \right)^2}} \right) \cos(2\pi f t) \quad (2.18)$$

$$\mathcal{E}_{V2} = A2\pi f * \frac{\mu_0 W}{2\pi} \sum_{i=1}^{\frac{N}{2}} \ln \left(\frac{\sqrt{\left(R * \cos\left(\pi + \frac{(\pi)(i-1)}{\left(\frac{N}{2}\right)-1} \right) - d \right)^2 + \left(R \sin\left(\pi + \frac{(\pi)(i-1)}{\left(\frac{N}{2}\right)-1} \right) + g/2 \right)^2}}{\sqrt{\left(r * \cos\left(\pi + \frac{(\pi)(i-1)}{\left(\frac{N}{2}\right)-1} \right) - d \right)^2 + \left(r \sin\left(\pi + \frac{(\pi)(i-1)}{\left(\frac{N}{2}\right)-1} \right) + g/2 \right)^2}} \right) \cos(2\pi f t)$$

(2.19)

Where, d is the in displacement of the conductor away from the centre and towards the gap.

A is the amplitude of applied current.

f is the frequency of applied current.

g is the gap between the two cores.

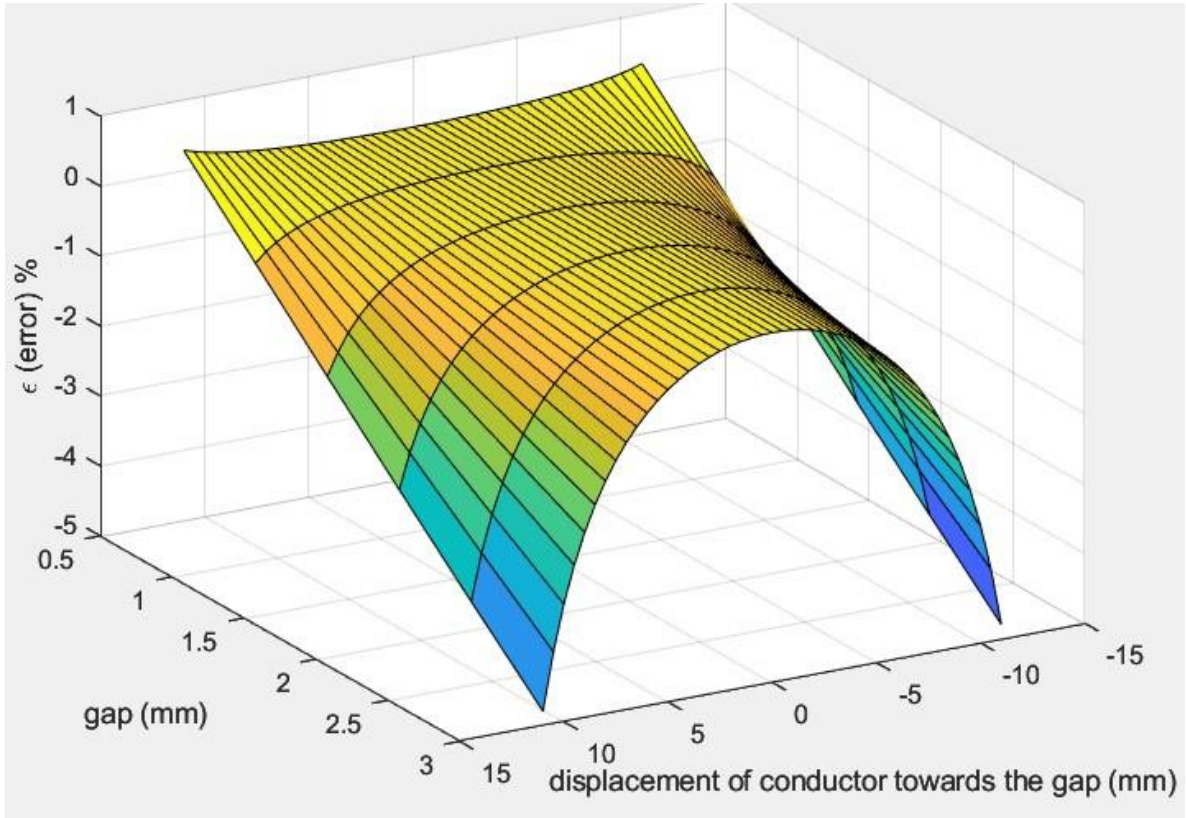
R & r are the outer and inner radius of the coil.

To calculate the error induced due to a given gap g, we calculate the sum of induced voltages at d = 0 and compare it with the voltage induced when the conductor is kept close to the gap (d ≠ 0).

$$\epsilon = \frac{(\epsilon_{v1} + \epsilon_{v2}) - (\epsilon_{v1@d=0} + \epsilon_{v2@d=0})}{(\epsilon_{v1@d=0} + \epsilon_{v2@d=0})} \quad (2.20)$$

Plotting eq. (2.20) for R = 20 mm, r = 13.25 mm, w = 3 mm and amplitude of A.C. current 2.5

A we get the following result.



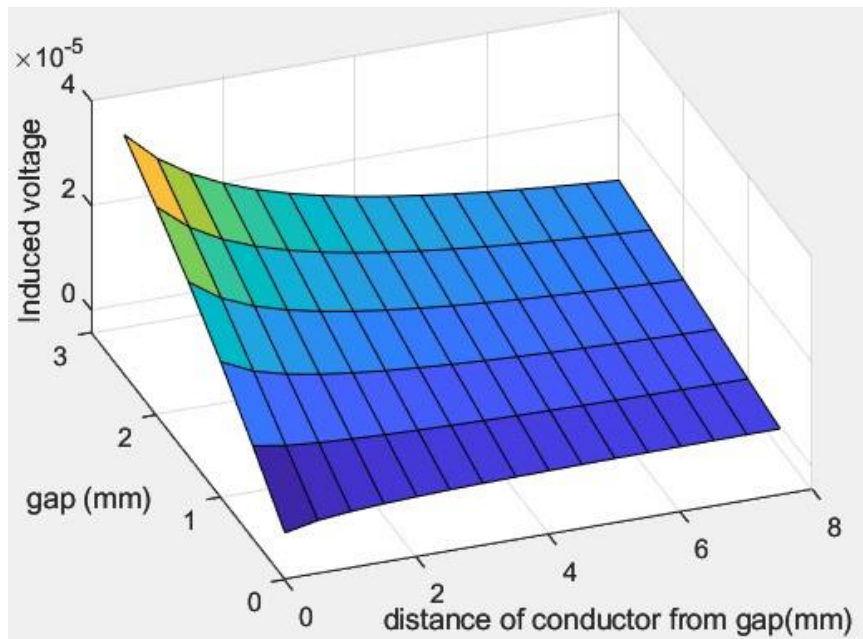
Graph 2.19: Error due to gap in split core Rogowski coil

To find the voltage induced by a wire near the gap substitute d = d+R in eq. (2.18) and eq. (2.19) as shown below.

$$\epsilon_{V1} = A2\pi f * \frac{\mu_0 W}{2\pi} \sum_{i=1}^{\frac{N}{2}} \ln \left(\frac{\sqrt{\left(R * \cos\left(\frac{(\pi)(i-1)}{\left(\frac{N}{2} \right) - 1} \right) - (d+R) \right)^2 + \left(R \sin\left(\frac{(\pi)(i-1)}{\left(\frac{N}{2} \right) - 1} \right) + g/2 \right)^2}}{\sqrt{\left(r * \cos\left(\frac{(2\pi-g)(i-1)}{\left(\frac{N}{2} \right) - 1} \right) - (d+R) \right)^2 + \left(r \sin\left(\frac{(\pi)(i-1)}{\left(\frac{N}{2} \right) - 1} \right) + g/2 \right)^2}} \right) \cos(2\pi f t)$$

$$\epsilon_{V2} = A2\pi f * \frac{\mu_0 W}{2\pi} \sum_{i=1}^{\frac{N}{2}} \ln \left(\frac{\sqrt{\left(R * \cos\left(\pi + \frac{(\pi)(i-1)}{(N/2)-1} \right) - (d+R) \right)^2 + \left(R \sin\left(\pi + \frac{(\pi)(i-1)}{(N/2)-1} \right) + g/2 \right)^2}}{\sqrt{\left(r * \cos\left(\pi + \frac{(\pi)(i-1)}{(N/2)-1} \right) - (d+R) \right)^2 + \left(r \sin\left(\pi + \frac{(\pi)(i-1)}{(N/2)-1} \right) + g/2 \right)^2}} \right) \cos(2\pi f t)$$

plotting the induced voltage for the same dimensions of the coil we get a result shown in Graph 2.20. The result is very similar to graph 2.12, but the induced voltages are higher because of the higher thickness of the given split core coil.



Graph 2.20: Induced voltage due to conductor near gap

Note: The distance between the gap and the conductor is measured from the outer diameter of the coil.

2.3.2 By finite element modelling

By following the steps as discussed in section 2.2.2, We can create another finite element model for the split core Rogowski coil. However, in this case we have to create 2 separate windings to represent the 2 halves of the split core coil as shown in the figure below.

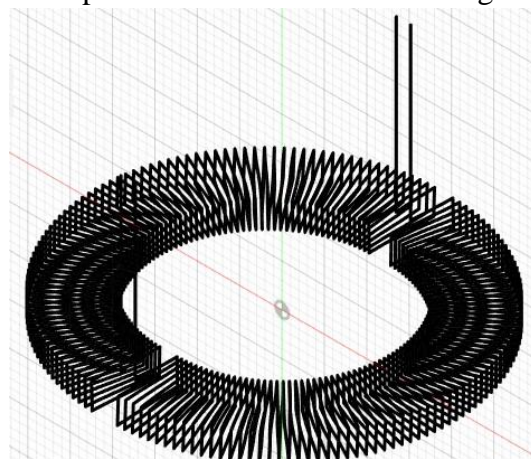


Figure 2.42- Geometric representation of split core Rogowski coil

The second winding is created by mirroring the first winding through the x plane as shown in the figure below.

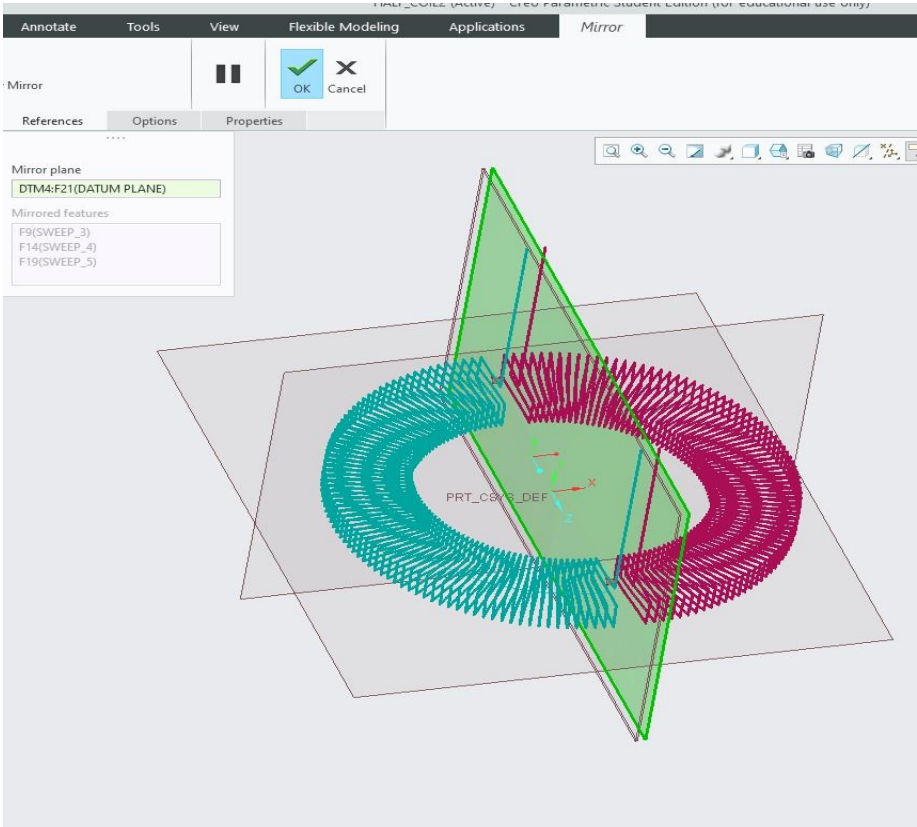


Figure 2.43: Creating second half using mirror command

the gap was measured to be between 1 to 2 mm. hence, the mirror plane is placed at a distance of 0.75 mm from the right most plane to create a gap of 1.5 mm as shown in the figure below.

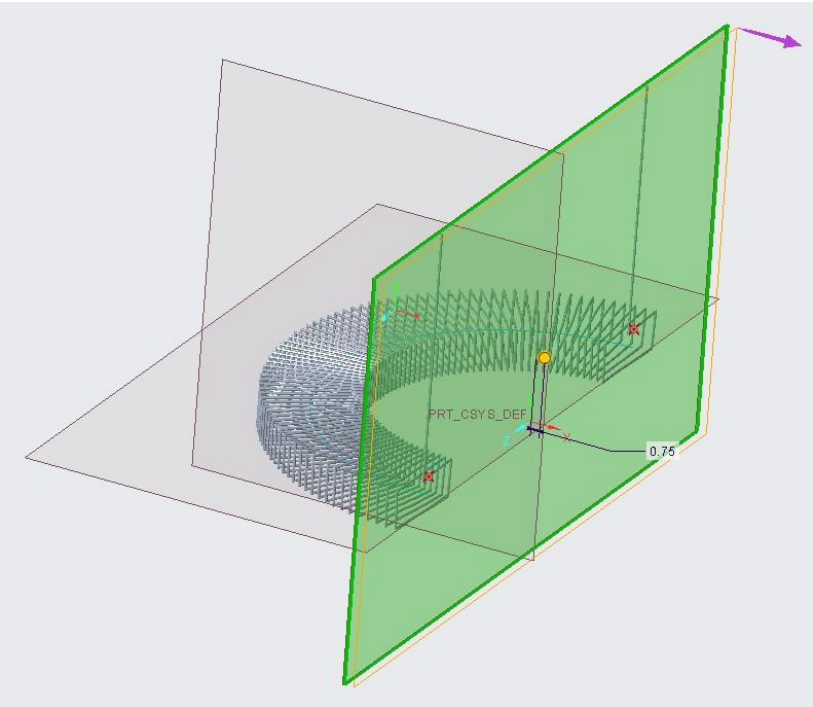


Figure 2.44: Mirror plane

The final geometry after converting to “.step” format, importing to Ansys maxwell and placing primary conductor placed in the centre of the coil is shown in the figure below.

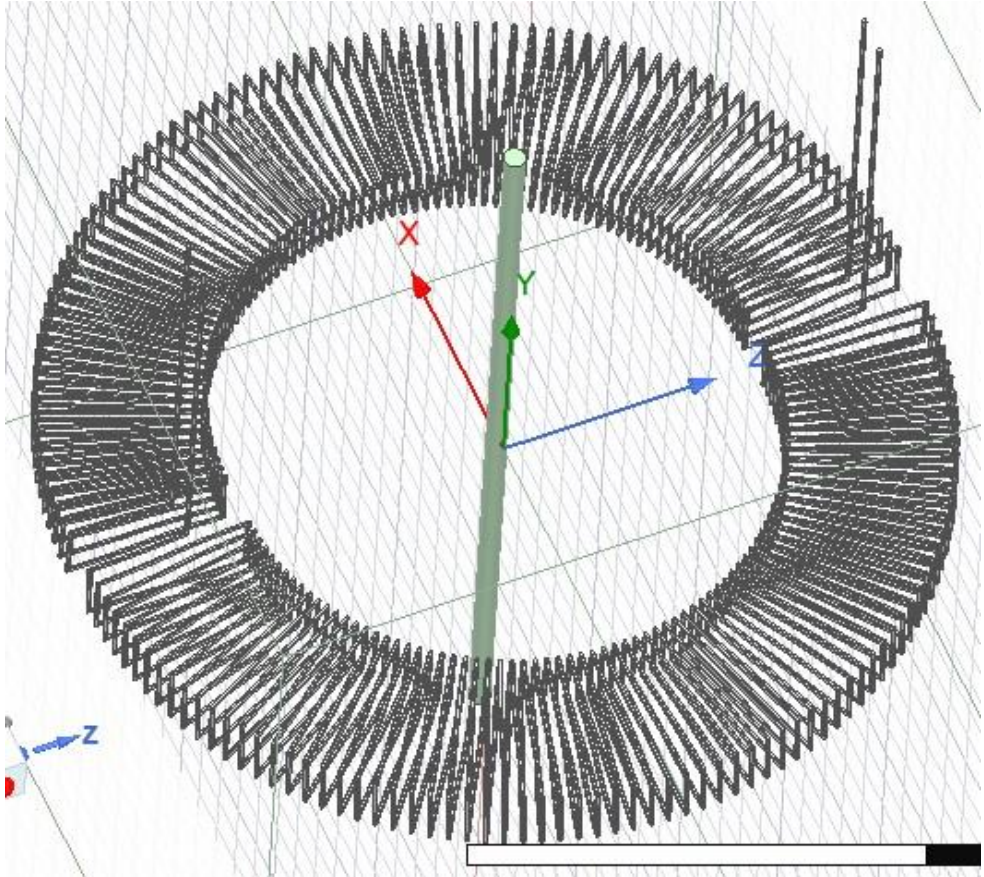


Figure 2.45: Final geometry for analysis

We added 3 windings and the coil terminals for each of these windings are shown in the figures below.

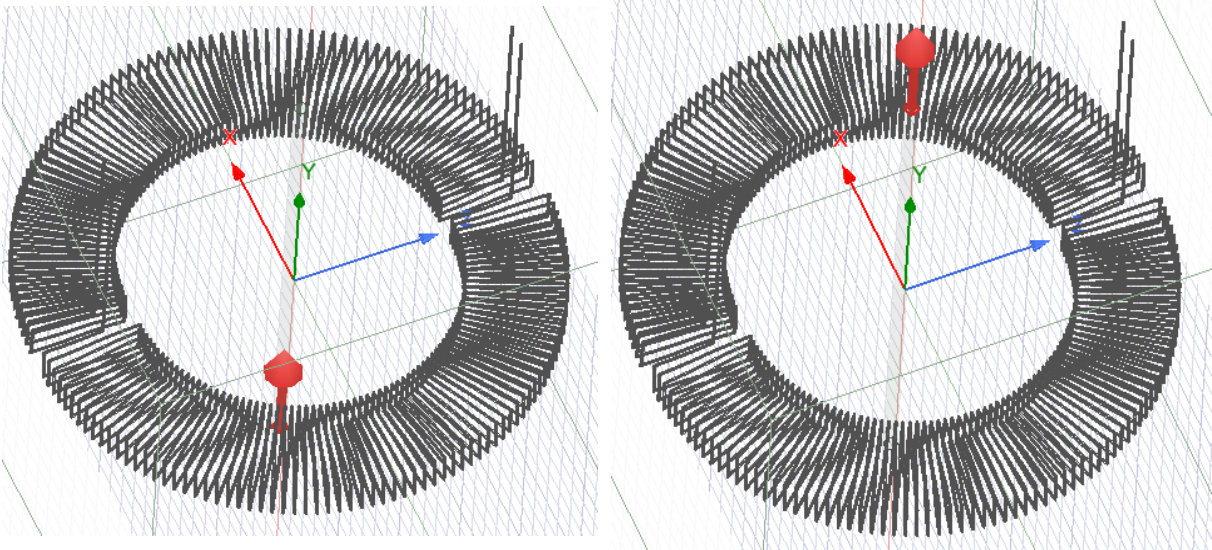


Figure 2.46: Coil terminals for winding

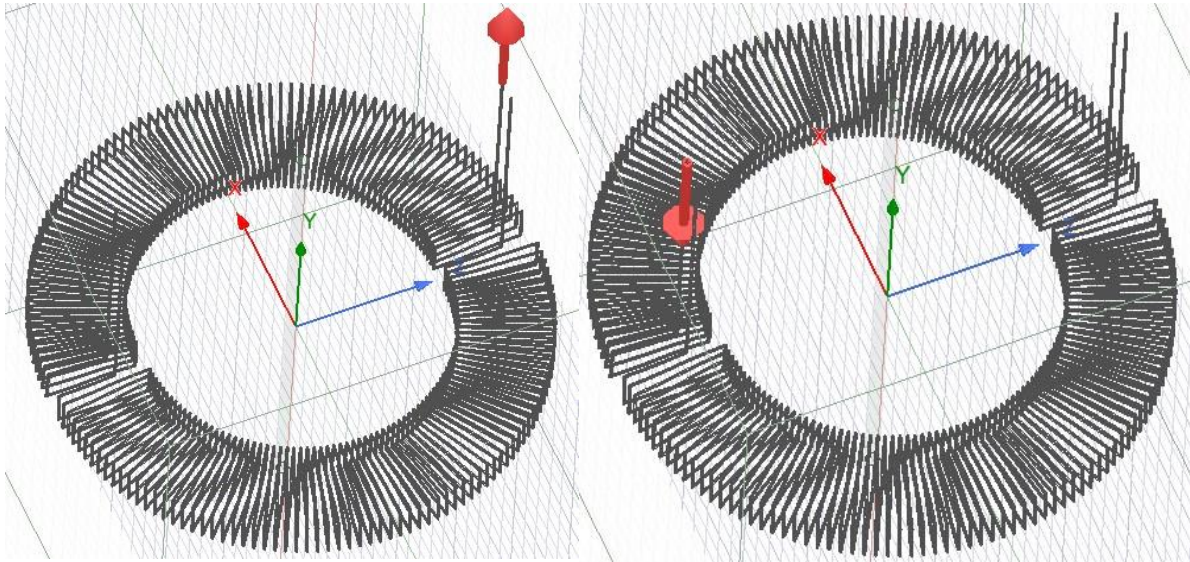


Figure 2.47: Coil terminals for winding 2

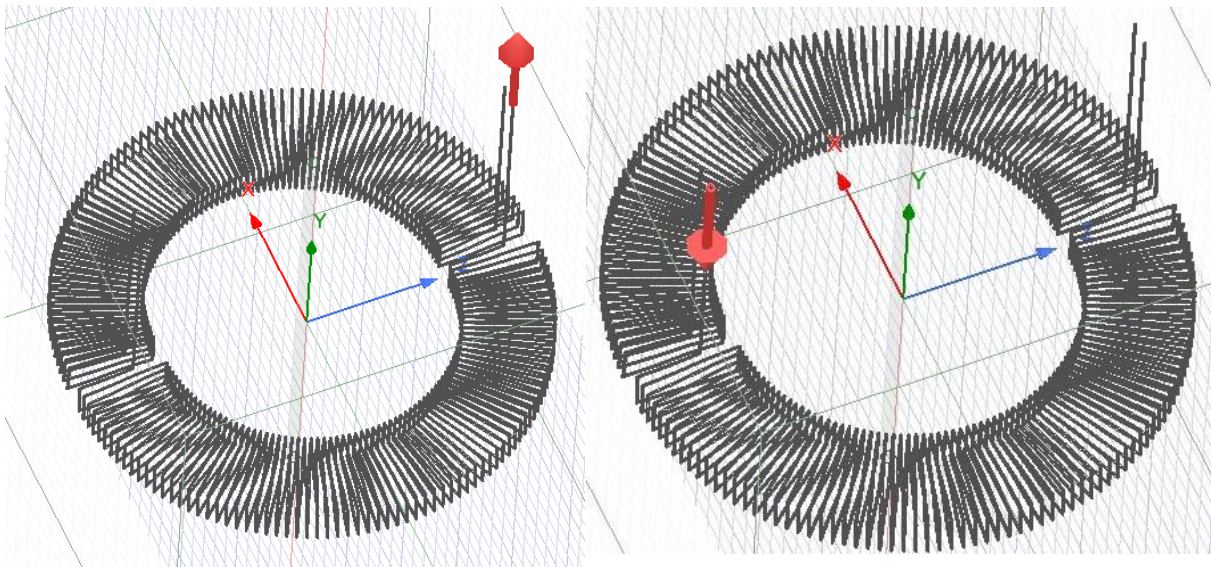
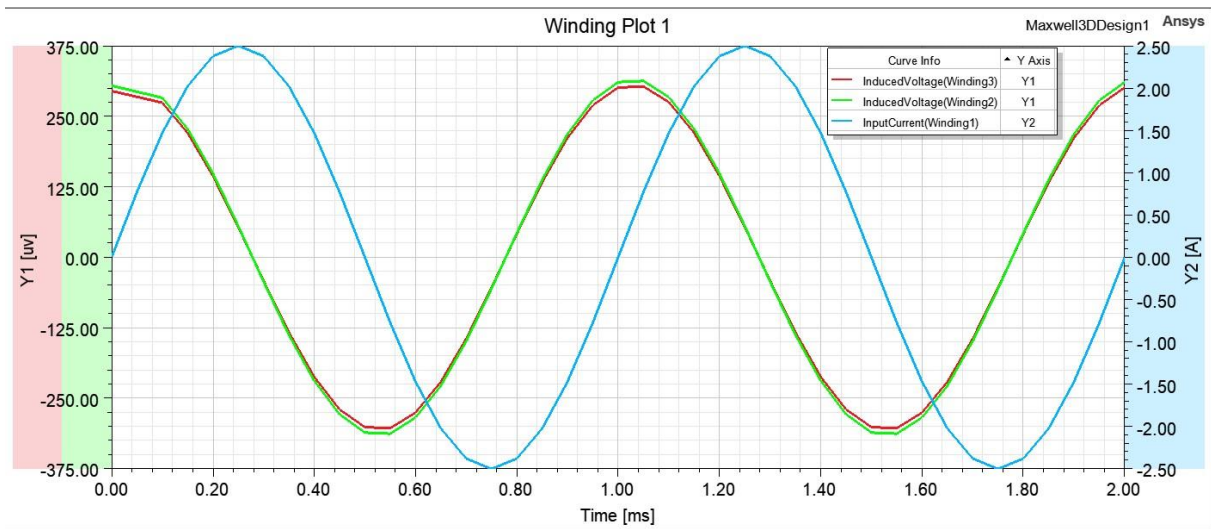


Figure 2.48: Coil terminals for winding 3

The result of this simulation is shown in the graph below.



Graph 2.21: Induced voltage in the 2 windings when the conductor is in the centre

From the above graph 2.21

Peak induced voltage = 302.90 + 312.57 = 615.48 uV , $V_{RMS} = 442.60$ uV.

Peak induced voltage calculated using eq. (2.18) and eq. (2.19) = 572.64 uV.

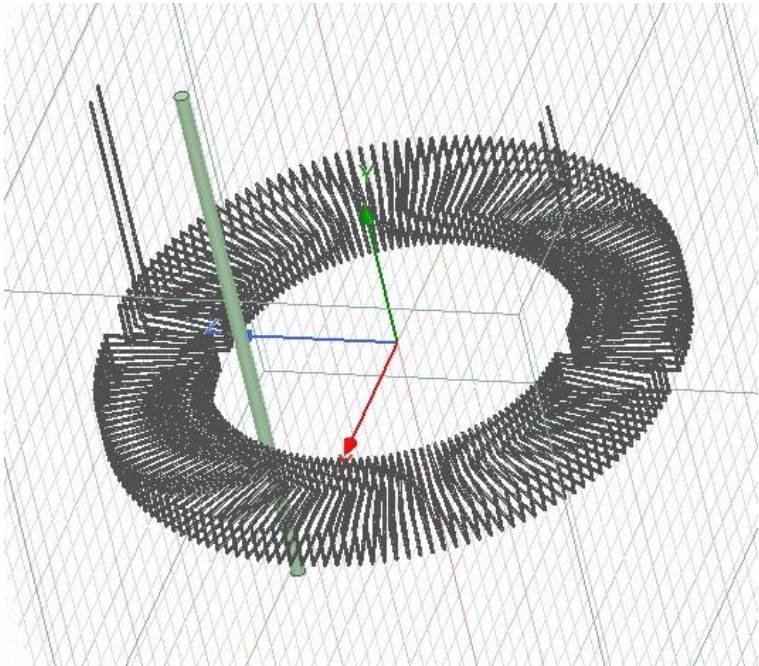
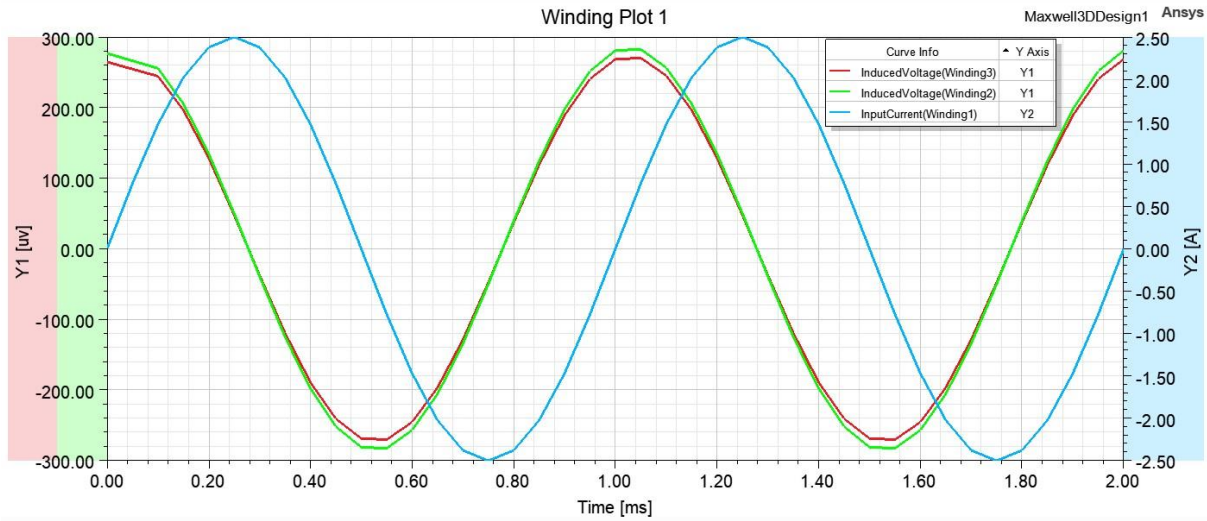


Figure 2.49: Conductor moved near gap

Now we move the primary conductor close to the gap by 11 mm as shown in the figure 2.49.

The result of this analysis is shown in the graph below.



Graph 2.22: voltage induced in each winding when the conductor is near the gap

As shown in the graph

Peak induced voltage = 270.13 + 282.54 = 552.68 uV, $V_{RMS} = 397.67$ uV.

Therefore, error induced due to gap $\epsilon = \left(\frac{552.68 - 615.48}{615.48} \right) * 100 = -10.2\%$

error calculated based on analytical formula using eq. (2.20) = - 1.773%

2.3.3 Experimental measurement of error

The experimental setup used to measure the error is same as what is described in section 2.2.3. the only difference is that the split core coil is mounted on the C.N.C. bench as shown in the figure below.

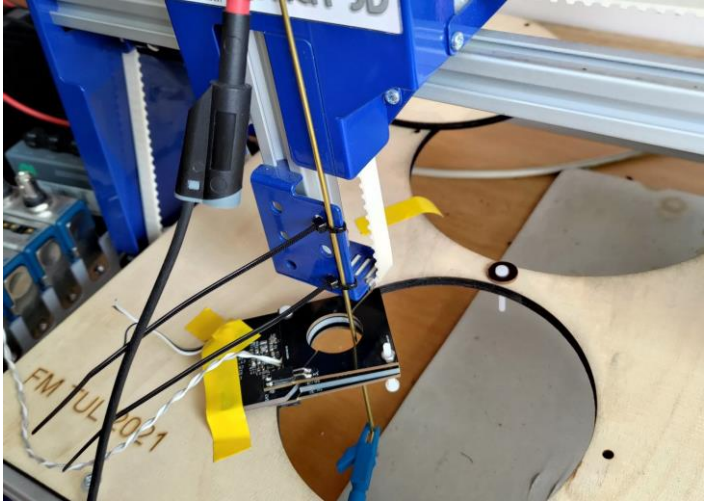
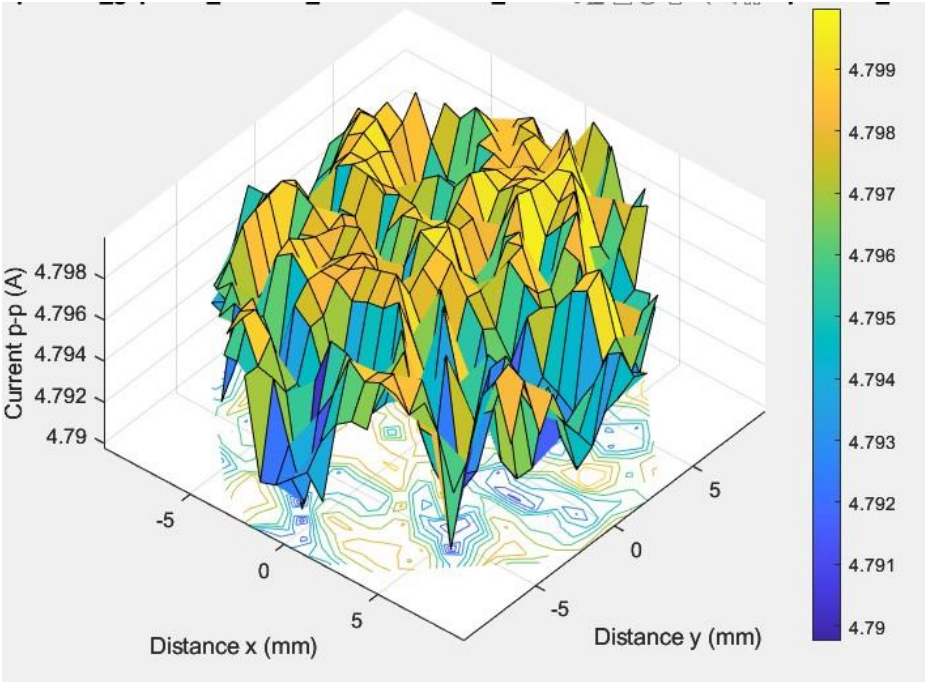


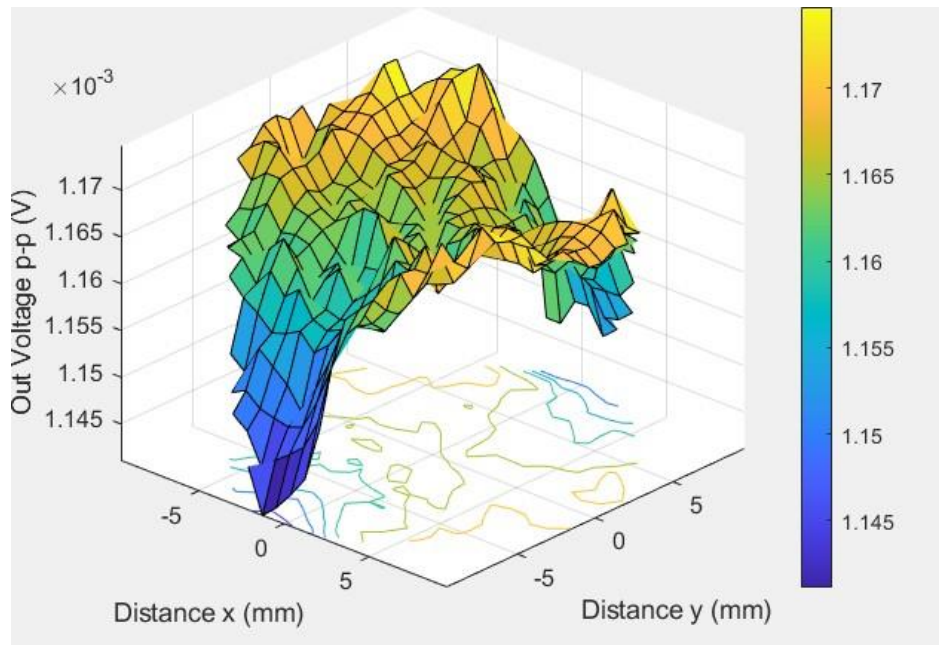
Figure 2.50: Split core coil mounted on the C.N.C. bench

Results:

The induced voltage and primary current measured at different positions of the primary conductor are shown in the graphs below.

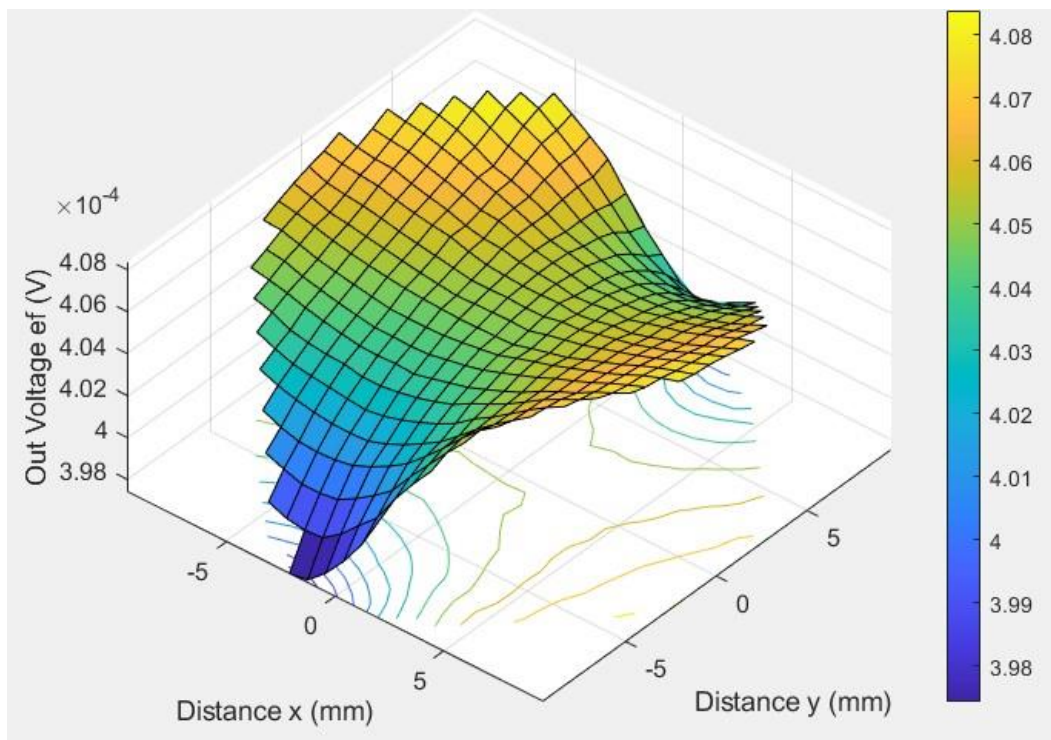


Graph 2.23: Primary current measured at different primary conductor positions (peak to peak)



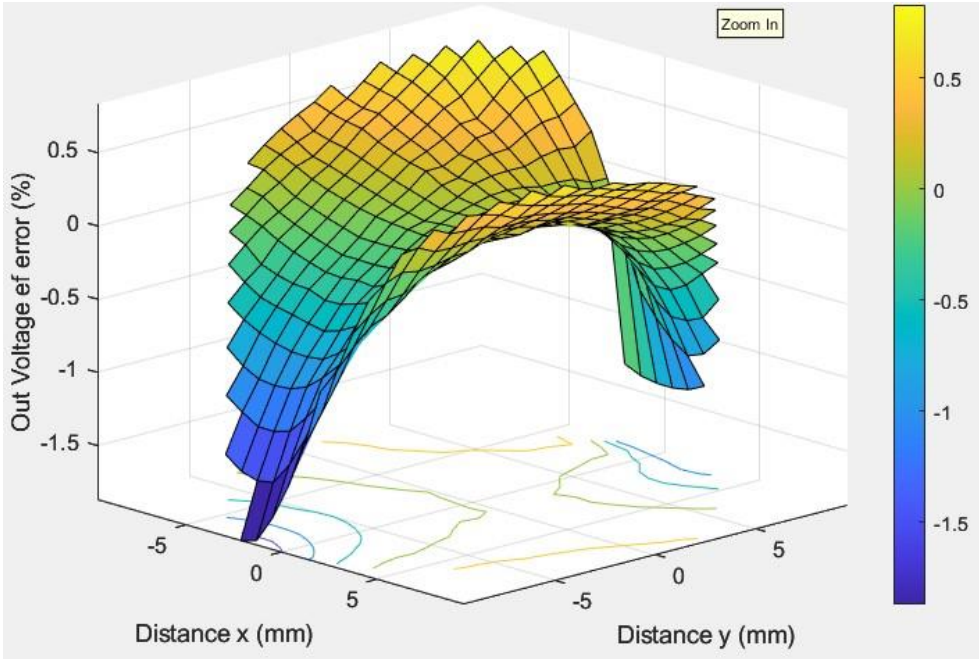
Graph 2.24: Induced voltage measured at different primary conductor positions (peak to peak)

As we can see from the above graphs the measurements are again affected by noise, hence we calculate the root mean square voltage at every point and then use these values to find the error.



Graph 2.25: Root mean square voltage calculated at different positions of the primary conductor

The error calculated at every point based on V_{RMS} is shown in the graph below.



Graph 2.26: error calculated for different position of the primary conductor

The experimental results show that the error is maximum when the conductor is closest to the gap, and it is measured to be about 1.87%.

Hall sensor

The Hall sensor is named after the American physicist Edwin Hall who first discovered the effect of a magnetic field on a current carrying conductor. He discovered that there is a potential difference (the Hall voltage) across an electrical conductor that is transverse to an electric current in the conductor and to an applied magnetic field perpendicular to the current[1]. The main cause of this effect is the **magnetic force component** of the Lorentz force equation given below:

$$\vec{F} = q\vec{E} + q(\vec{v} \times \vec{B}) \quad (3.10)$$

Where, q is the charge on the particle ($= -1.60217663 \times 10^{-19}$ C for an electron)

\vec{v} is the velocity of the charged particle

The Lorentz force equation can be used to calculate the net force acting on a charged particle moving through an electric and/or magnetic field. From the above equation, it is clear that the amount of magnetic force (FB) acting on a charged particle depends on the velocity of the charged particle and magnetic field in which the particle is moving.

$$|\vec{F}_B| = q |\vec{v}| |\vec{B}| \sin(\theta)$$

Where, θ is the angle between the velocity of the particle and the magnetic field.

from the above equation, it is important to note that the amount magnetic force acting on the charged particle also depends on the angle between the velocity vector and the magnetic field vector.

We can get a clear understanding of the Hall effect from the figures below

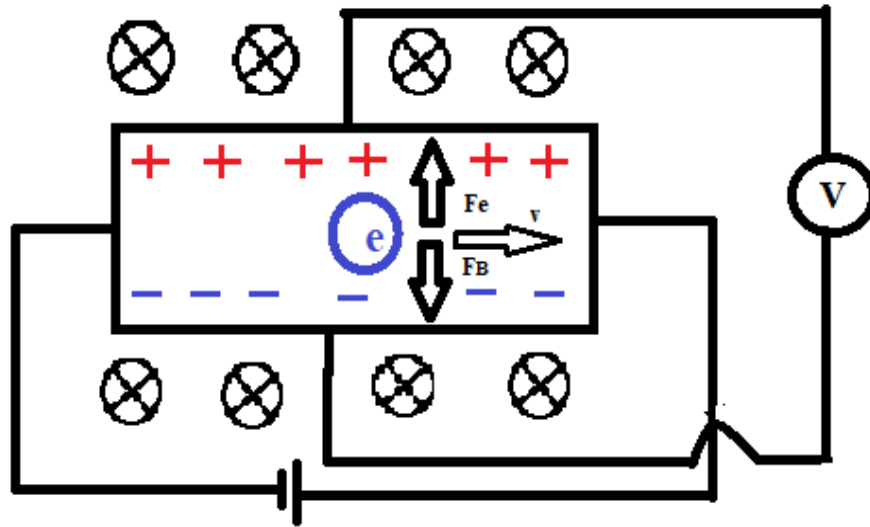


Figure 3.10: Hall effect

The figure shown above shows the forces acting on an electron in the Hall sensing element. Initially only the magnetic force (F_B) acts on the electron. Assuming that the magnetic field is perpendicular to the face of the sensing element, the magnetic force (F_B) acts in the downward direction as shown in the figure. Over a period of time as the electron density increases on the lower side of the sensing element, the potential difference is created between the lower & upper half of the sensing element. This potential difference creates an electric field which pushes the electron in the upward direction with force (F_E) as shown in the figure. The force F_E increases with the increasing potential difference and finally becomes equal to F_B . At this point we get a constant measurable voltage between the upper and lower half of the sensing element. This voltage is known as the Hall e.m.f. (\mathcal{E}_H). We can calculate \mathcal{E}_H as shown below.

$$\text{We know that, } \mathcal{E}_H = |\vec{E}| * W \quad (3.11)$$

where, W is the width of the conductor.

$$\because F_E = -F_B$$

$$\because q\vec{E} = -q(\vec{v} \times \vec{B}) \quad (3.12)$$

$$|\vec{E}| = |\vec{v}| * |\vec{B}| \sin(\theta) \quad (3.13)$$

Let the current flowing through the sensing element be I, we know that:

$$I = nq |\vec{v}| * A \quad (3.14)$$

Where, n is the charge density of the material i.e., number of free electrons/cubic meter. It is material property.

$n = 8.49 * 10^{28}$ electrons/m³ for copper.

A is the cross-sectional area perpendicular to the direction of flow of current. $A = W * t$.

t is the thickness of the sensing element.

Substituting the value of $|\vec{v}|$ from eq. (3.14) in eq. (3.13)

$$|\vec{E}| = \frac{I}{nqA} * |\vec{B}| \sin(\theta) \quad (3.15)$$

Substituting eq. (3.15) in eq. (3.11),

$$\epsilon_H = \frac{I}{nqA} * |\vec{B}| \sin(\theta) * W = \frac{I}{nqt} * |\vec{B}| \sin(\theta) \quad (3.16)$$

From eq. (3.16) we can see a directly proportional relationship between ϵ_H and the magnitude of magnetic field. This relationship is used to estimate the strength of the magnetic field which is in turn used to estimate the current flowing in the primary conductor using Biot-Savart's law. However, it is important to note that the amount of Hall voltage induced in the sensor depends on the distance between the sensing element and the primary current carrying conductor. From eq. (3.16) we can also see that ϵ_H also depends on θ , which is the angle between the velocity vector, i.e., the vector in the direction of applied electric field and the magnetic field. Therefore, we can conclude that The current measured by the Hall sensor is also susceptible to changes in geometric parameters just like the Rogowski coil.

3.1 Error study of Hall sensor

From eq. (1.4) we know that \vec{B} is inversely proportional r. i.e., the magnetic field reduces if the distance between the primary conductor & the sensing element increases. This means that if the primary conductor cannot be placed precisely, at a known particular distance from the sensing element, then the induced Hall voltage cannot be used to accurately estimate the amount of current flowing in the primary conductor. We can compensate for this error by surrounding the

primary conductor with multiple sensing elements. An example for this type of Hall sensor is shown in the figures below.



Figure 3.11: Hall sensor with multiple sensing elements

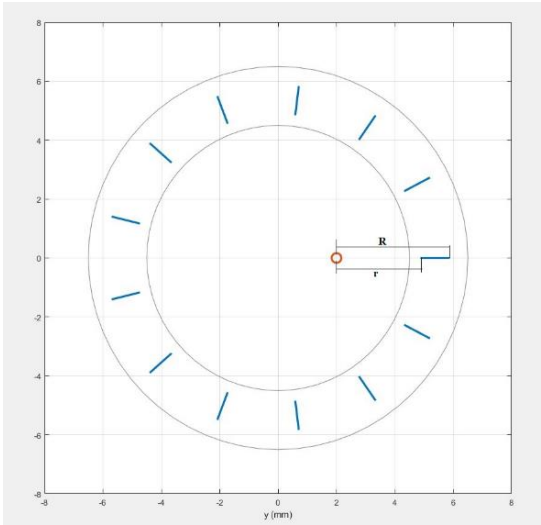


Figure 3.12: Equivalent schematic diagram

Figure 3.12 shows the equivalent schematic diagram for the sensor. The orange circle represents the misplaced primary conductor and the blue lines represent the sensing elements. Ideally, the primary conductor should be placed exactly in the centre and the Hall voltage induced in every sensing element will be the same. Therefore, the total induced voltage is the voltage induced in one sensing element multiplied by the total number of sensing elements. However, as we can see in this case, if the conductor moves away from the sensors on the left it also moves closer to the sensors on the right. Hence, the drop in the induced voltages on the left is somewhat compensated by the increase in the induced voltages on the right. However, this compensation is not perfect and the final induced voltage is still different from voltage induced if the primary conductor is exactly in the centre. This difference depends on the displacement of the primary conductor from the centre and the number of sensing elements surrounding the conductor. In the upcoming sections we have again estimated this error with the help of analytical formulae and verified our results with a finite element model and physical experiments.

3.1.1 Estimation of error using analytical formulae

We need:

$$error(\epsilon) = f(N, d, r, R)$$

Where, N is the number of sensing elements.

d is the displacement of the conductor with respect to the centre.

r is the distance between the primary conductor & the closer end of the sensor. i.e., the inner radius if the conductor is exactly in the centre.

R is the distance between the primary conductor and the further end of the sensor. i.e., the outer radius if the conductor is placed exactly in the centre

Assumptions:

- Wire is of infinite length.
- Wire has negligible diameter

We know that,

$$\epsilon = \frac{\mathcal{E}_{H(disp)} - \mathcal{E}_{H(centre)}}{\mathcal{E}_{H(centre)}}$$

From eq. (3.16),

$$\mathcal{E}_{H(centre)} = N * \frac{I|\vec{B}|}{nqt} \quad \& \quad \mathcal{E}_{H(disp)} = \sum_{i=1}^N \frac{I|\vec{B}_i|}{nqt}, \text{ Assuming } \theta = 90^\circ$$

$|\vec{B}|$ is not constant over the length of the sensing element, however, we can get a decent approximation of mean flux density from the formula below:

$$|\vec{B}| = \frac{\phi}{A}$$

Where, ϕ is the total magnetic flux flowing through the sensing element.

A is the area of the face perpendicular to the magnetic field.

$$\therefore \epsilon = \frac{(\sum_{i=1}^N \frac{I\phi_i}{nqtA}) - \frac{NI\phi}{nqtA}}{\frac{NI\phi}{nqtA}}$$

After simplifying the above equation, we get

$$\epsilon = \frac{(\sum_{i=1}^N \phi_i) - N\phi}{N\phi} \quad (3.17)$$

For a given sensing element;

$$\phi = \int_r^R \vec{B} \cdot dA = \int_r^R \frac{\mu_0 I_p W}{2\pi x} dx = \frac{\mu_0 I_p W}{2\pi} \ln\left(\frac{R}{r}\right) [2] \quad (3.18)$$

where, w is the thickness of the sensing element.

Substituting eq. (3.18) in eq. (3.17);

$$\epsilon = \frac{(\sum_{i=1}^N \frac{\mu_0 i p W}{2\pi} \ln(\frac{R_i}{r_i})) - N(\frac{\mu_0 i p W}{2\pi} \ln(\frac{R}{r}))}{N(\frac{\mu_0 i p W}{2\pi} \ln(\frac{R}{r}))} \quad (3.19)$$

Where, R_i & r_i are the perpendicular distance between the conductor and the inner and outer side of each sensor.

$$R_i = \sqrt{(R * \cos(2\pi i/N) - d)^2 + (R \sin(2\pi i/N))^2}$$

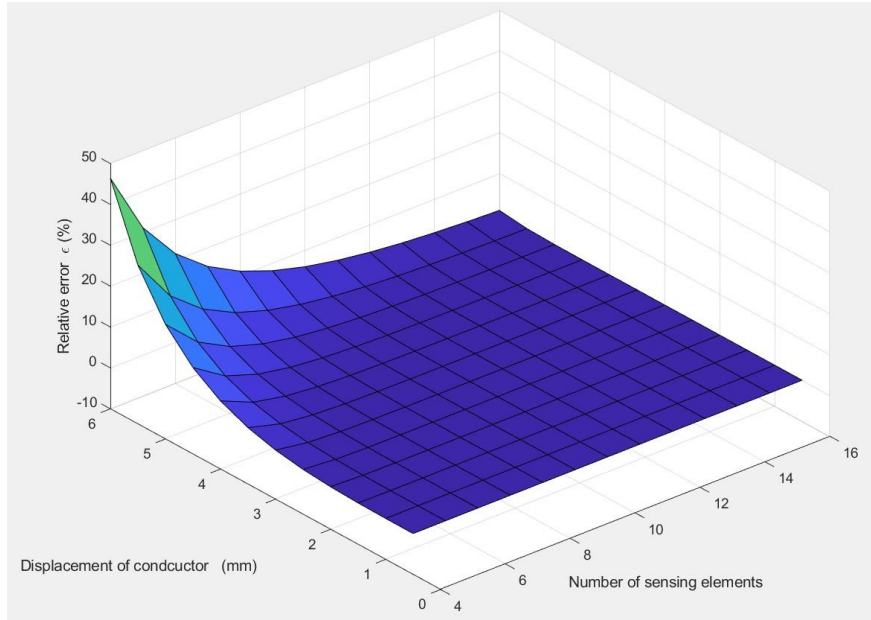
$$r_i = \sqrt{(r * \cos(2\pi i/N) - d)^2 + (r \sin(2\pi i/N))^2}$$

$$\therefore \epsilon = \frac{(\sum_{i=1}^N \frac{\mu_0 i p W}{2\pi} \ln(\frac{\sqrt{(R * \cos(2\pi i/N) - d)^2 + (R \sin(2\pi i/N))^2}}{\sqrt{(r * \cos(2\pi i/N) - d)^2 + (r \sin(2\pi i/N))^2}})) - N(\frac{\mu_0 i p W}{2\pi} \ln(\frac{R}{r}))}{N(\frac{\mu_0 i p W}{2\pi} \ln(\frac{R}{r}))}$$

Simplifying the above equation,

$$\epsilon = \frac{(\sum_{i=1}^N \ln(\frac{\sqrt{(R * \cos(2\pi i/N) - d)^2 + (R \sin(2\pi i/N))^2}}{\sqrt{(r * \cos(2\pi i/N) - d)^2 + (r \sin(2\pi i/N))^2}})) - N(\ln(\frac{R}{r}))}{N(\ln(\frac{R}{r}))} \quad (3.20)$$

We plotted the above function for $R = 8.25$, $r = 7.75$, $d = [0,6]$ and N increasing from 4 to 16.



Graph 3.1: Conductor displacement v/s number of sensing elements v/s error

It is important to note that eq. (3.20) assumes that the conductor is displaced only along the x-axis. If the conductor is displaced in some other direction, then the formula to calculate error will change as shown below.

$$R_i = \sqrt{(R * \cos(2\pi i/N) - d * \cos(\phi))^2 + (R \sin(2\pi i/N) - d * \sin(\phi))^2}$$

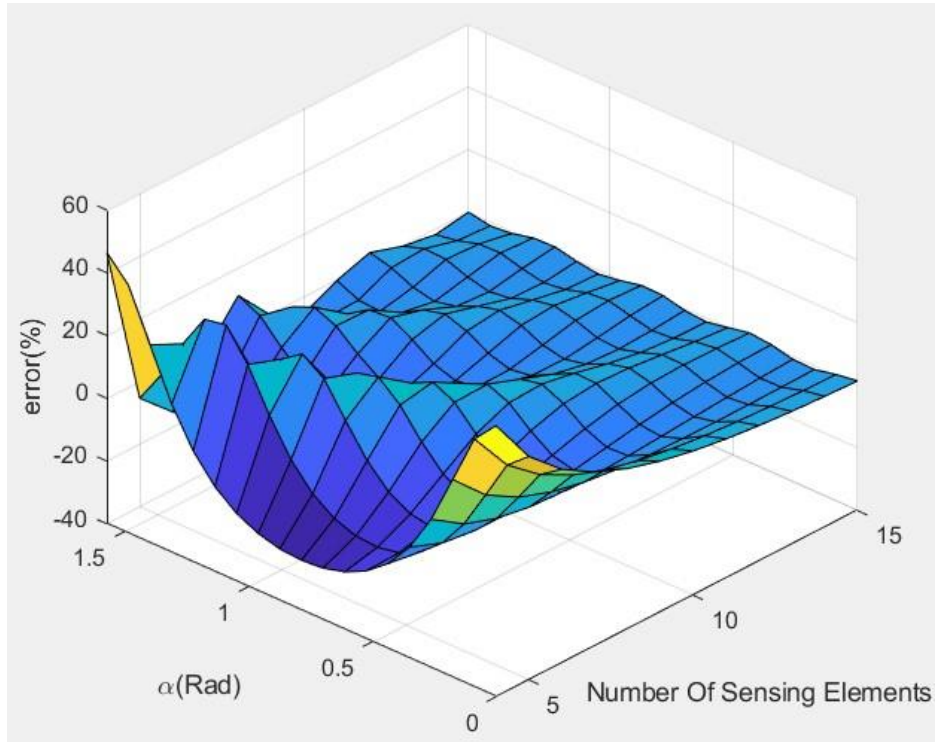
$$r_i = \sqrt{(r * \cos(2\pi i/N) - d * \cos(\phi))^2 + (r \sin(2\pi i/N) - d * \sin(\phi))^2}$$

Where ϕ is the angle between the direction of displacement and x-axis.

Substituting the values of R_i and r_i eq. (3.19) is modified as:

$$\epsilon = \frac{(\sum_{i=1}^N \ln(\frac{\sqrt{(R * \cos(2\pi i/N) - d * \cos(\phi))^2 + (R \sin(2\pi i/N) - d * \sin(\phi))^2}}{\sqrt{(r * \cos(2\pi i/N) - d * \cos(\phi))^2 + (r \sin(2\pi i/N) - d * \sin(\phi))^2}})) - N(\ln(\frac{R}{r}))}{N(\ln(\frac{R}{r}))} \quad (3.21)$$

For a given value of $d = 6$ mm, if we plot the above function for $R = 8.25$, $r = 7.75$, $\alpha = [0, \pi/2]$ and N increasing from 4 to 16, we get the following result.



Graph 3.12: Alpha v/s number of sensing elements v/s error

using eq. (3.18) we can also calculate the net flux inducing a voltage in the sensor, due to a current carrying wire that is outside the sensor radius. When the current carrying wire is inside the sensor radius, the magnetic field direction on the left and right side of the current carrying wire are opposite to each other. Hence, each sensing element has to be oriented in such a way

that the voltage induced in all of them are positive. If the current carrying wire is placed outside the radius of the sensor, then the magnetic field will not flip completely in the two halves of the sensor. Hence, negative voltages are induced in some of the sensing elements. In an ideal condition this negative voltage should be equal to the positive voltage and the net induced voltage should be equal to zero. However, this compensation is not perfect and there is always a net induced voltage in some direction. The net flux due to a current carrying wire near the sensor is derived below.

$$\phi_T = \sum_{i=1}^N \frac{\mu_0 i_p W}{2\pi} \ln \left(\frac{R_i}{r_i} \right)$$

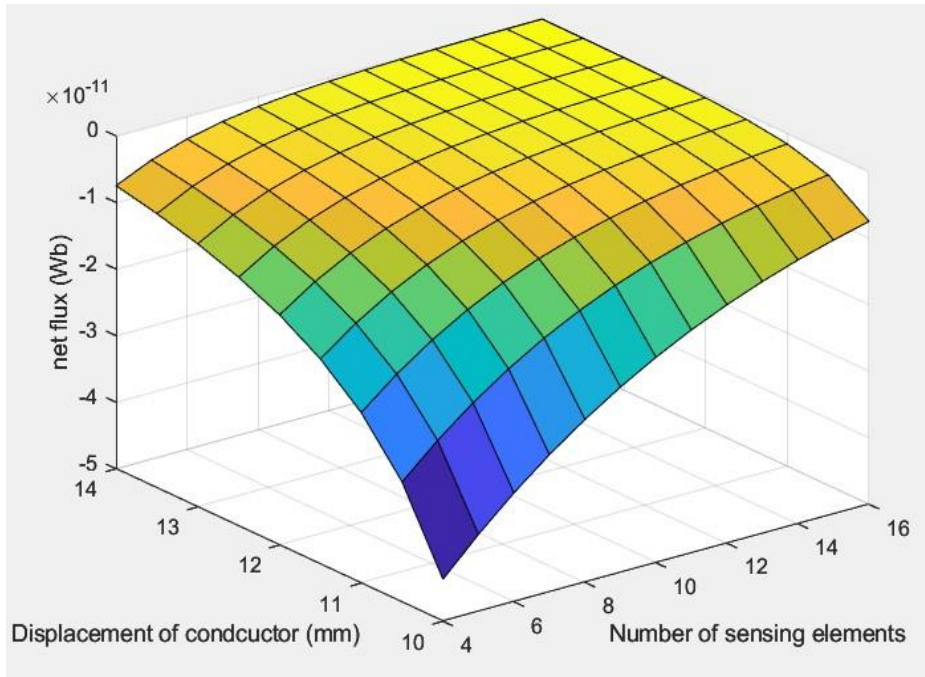
$$\text{Where, } R_i = \sqrt{(R * \cos(2\pi i/N) - (d + R))^2 + (R \sin(2\pi i/N))^2}$$

$$r_i = \sqrt{(r * \cos(2\pi i/N) - (d + R))^2 + (r \sin(2\pi i/N))^2}$$

d is the minimum distance between the conductor and the outer edge of the sensor.

$$\therefore \phi_T = \sum_{i=1}^N \frac{\mu_0 i_p W}{2\pi} \ln \left(\frac{\sqrt{(R * \cos(2\pi i/N) - (d + R))^2 + (R \sin(2\pi i/N))^2}}{\sqrt{(r * \cos(2\pi i/N) - (d + R))^2 + (r \sin(2\pi i/N))^2}} \right) \quad (3.22)$$

Plotting the above equations for the same values of R , r and current $i_p = 2.5$ A we get the following graph.



Graph 3.13: Conductor displacement ($d+R$) v/s no. of sensing elements v/s net flux.
Note: the primary is outside the sensor hole but the distance is measured from the centre of the sensor hole.

As we can see from graph 3.13, increasing the number of sensing elements is also helpful for reducing the induced voltage in the sensor, due to surrounding magnetic fields.

Error due to change in Θ :

From eq. (3.16) it is clear that \mathcal{E}_H also depends on $\sin(\Theta)$, where Θ is the angle between magnetic field and the applied electric field of the sensing element. From eq. (3.16) we can find the error for $\Theta \neq 90^\circ$ as shown below.

$$\epsilon_\theta = \frac{\mathcal{E}_H \sin(\theta) - \mathcal{E}_H}{\mathcal{E}_H}$$

$$\therefore \epsilon_\theta = \sin(\theta) - 1$$

If n = no. of tilted sensors & N = total no. of sensors, then the net error is given by:

$$\epsilon_\theta = \frac{n(\sin(\theta) - 1)}{N}$$

3.1.2 Estimation of error by finite element model

to verify our analytical results, we create a simple finite element model with a current carrying conductor and 4 surfaces as shown in the figure below.

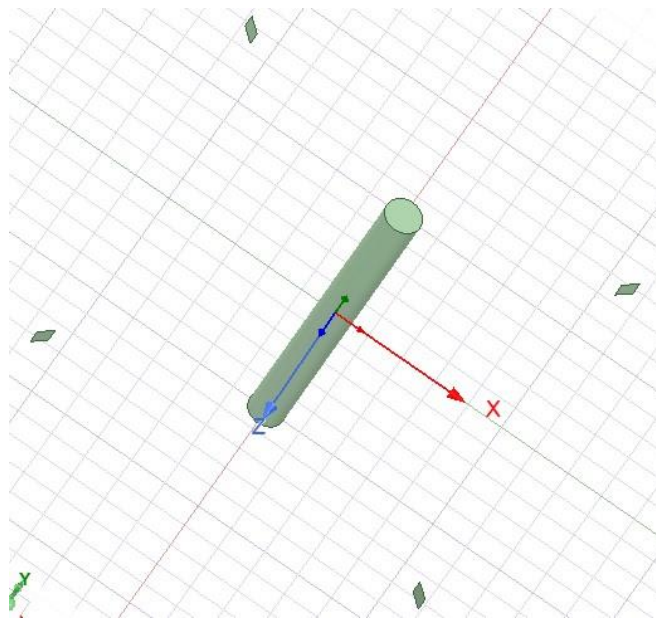


Figure 3.13: Geometry for analysis

Similar to previous analysis, a current of 2.5 A is applied to the primary conductor. After following similar steps as shown in previous analysis like creation of region etc. The total magnetic flux through the 4 surfaces is calculated using field calculator as shown in the figure below.

he total flux calculated = $6.359 \times 10^{-12} \text{ Wb}$

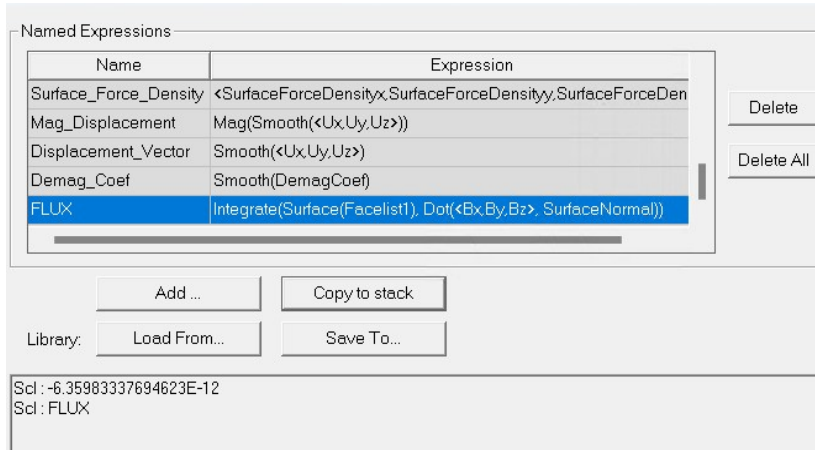


Figure 3.14: Total flux through the given 4 surfaces

From eq. (3.22) the total value of flux = $6.25 \times 10^{-11} \text{ Wb}$

Now we repeat the same analysis with the conductor moved 6 mm away from the centre.

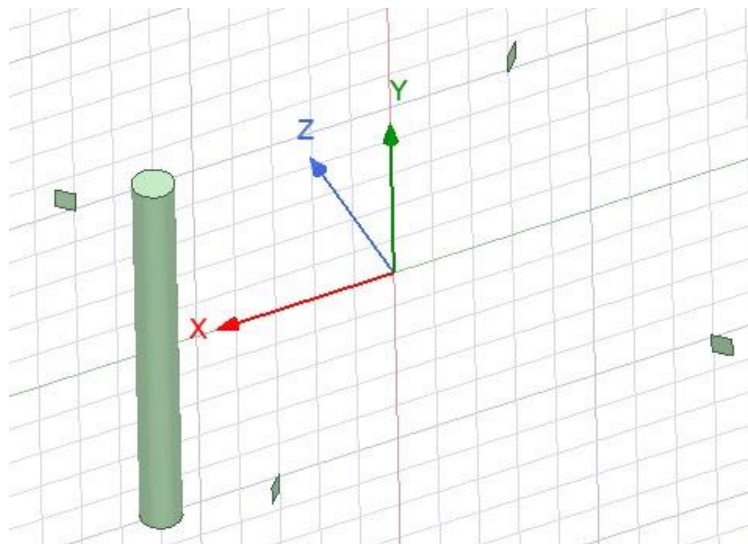


Figure 3.15: Conductor moved away from the centre

flux through the 4 surfaces was calculated to be $4.08 \text{E-}12 \text{ Wb}$ as shown below.

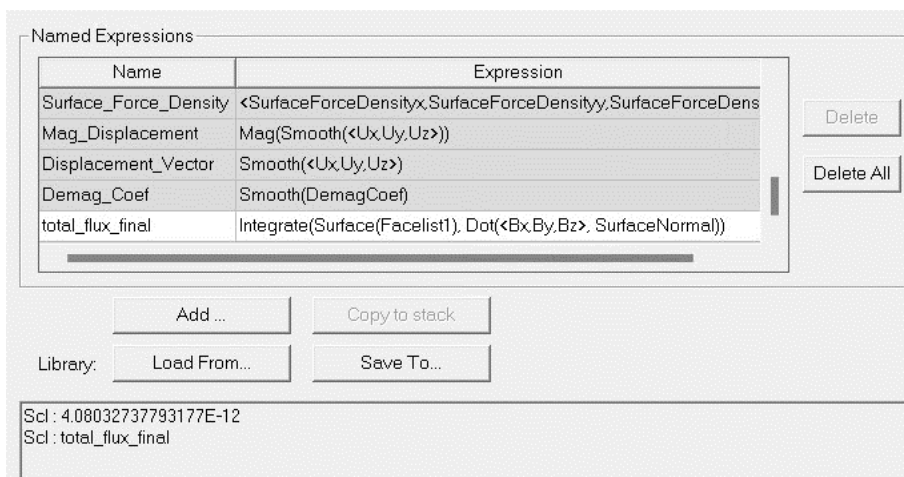


Figure 3.16: total flux for displaced conductor

$$\therefore \epsilon = \frac{4.08-6.359}{6.359} * 100 = -35.8\%$$

Error calculated using eq. (3.21)

$$\epsilon = \frac{(\sum_{i=1}^4 \ln \left(\frac{\sqrt{(8.25 \cdot \cos(2\pi i/4) - 6 \cdot \cos(\frac{\pi}{4}))^2 + (8.25 \cdot \sin(2\pi i/4) - 6 \cdot \sin(\frac{\pi}{4}))^2}}{\sqrt{(7.75 \cdot \cos(2\pi i/4) - 6 \cdot \cos(\frac{\pi}{4}))^2 + (7.75 \cdot \sin(2\pi i/4) - 6 \cdot \sin(\frac{\pi}{4}))^2}} \right)) - 4 \left(\ln\left(\frac{R}{r}\right) \right)}{\ln\left(\frac{8.25}{7.75}\right)} = -24.05\%$$

3.1.3 Experimental measurement of error

The experiment is conducted using the same setup as described in section 2.2.3. The Hall sensor with 4 sensing elements is mounted on the C.N.C. bench as shown in the figure below.

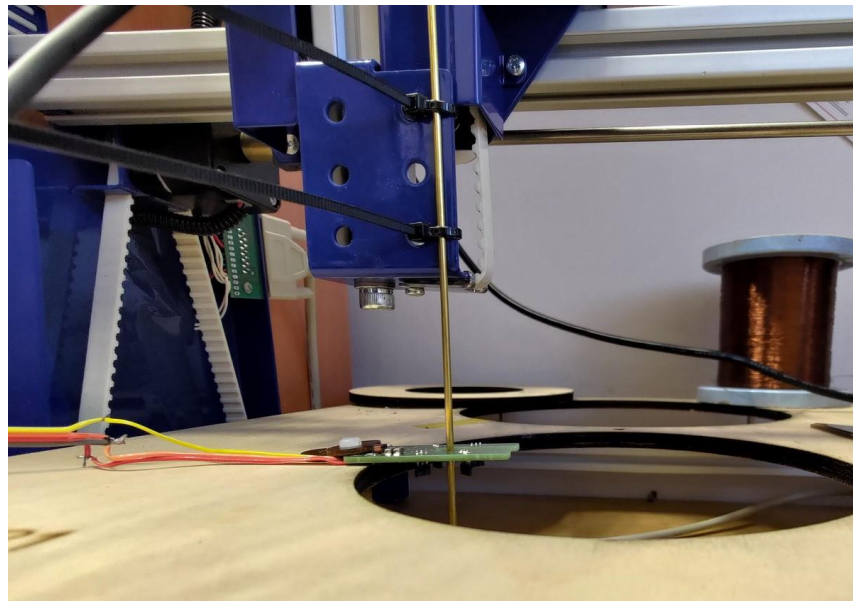


Figure 3.17: Hall sensor with 4 sensing elements mounted on the C.N.C bench

The sensor used for this experiment is shown in the figure below.

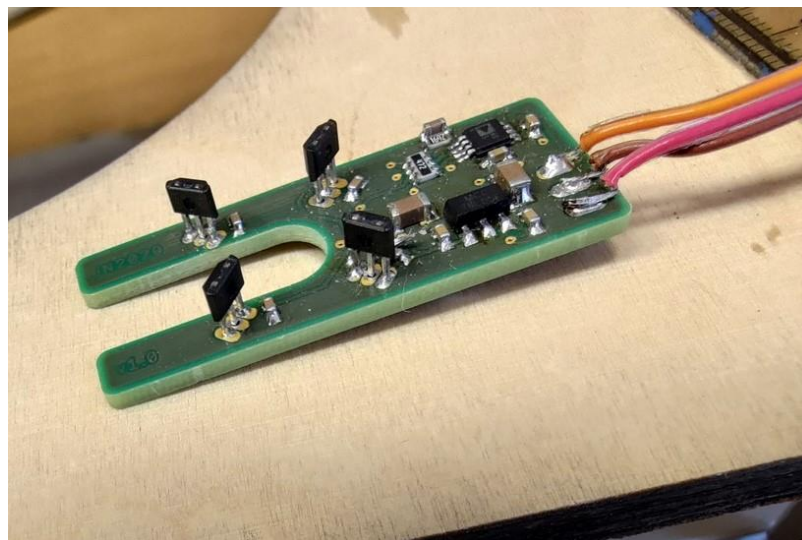
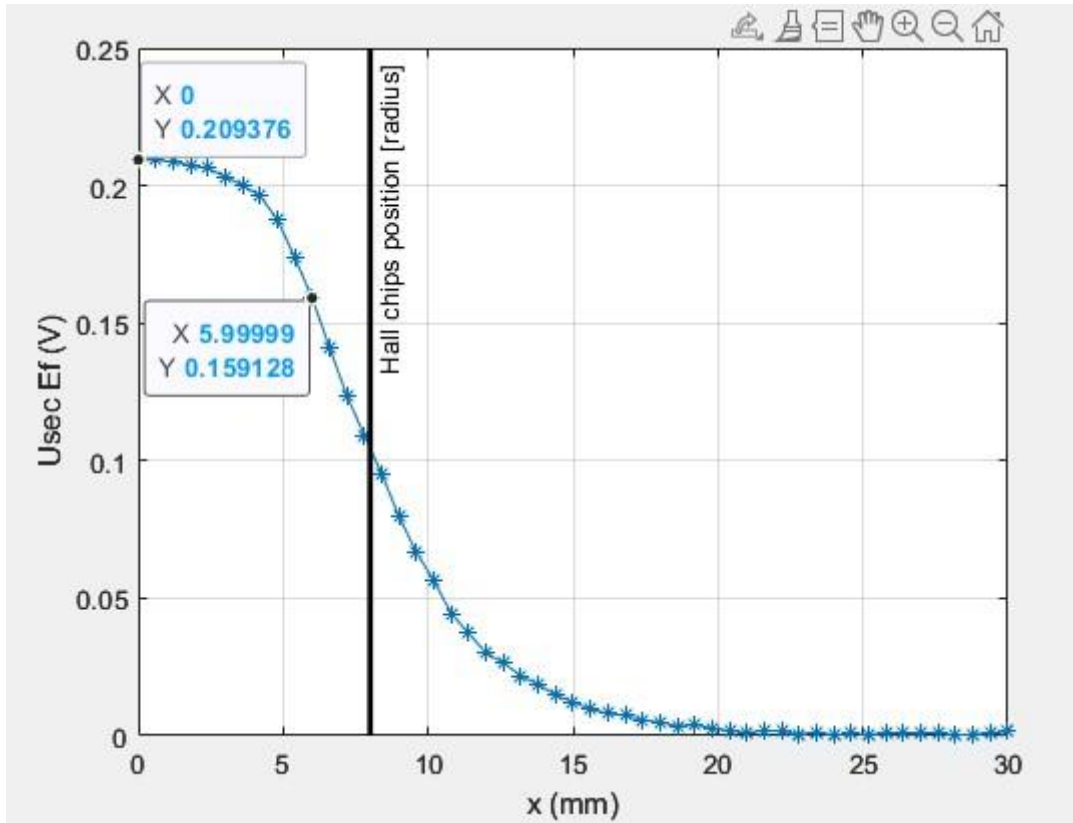


Figure 3.18: Hall sensor used for the experiment

Results:

The Hall sensor is more susceptible to noise as compared to the Rogowski coil since the induced voltage is a direct function of flux and not its derivative. Hence, to accurately measure the error we had to filter the measured induced voltage signal using discrete fourier transform in MATLAB. Inudced voltage after filtering out other unwanted frequencies is shown in the figure below.



Graph 3.14: Induced voltage measure at different distances from the centre

The measured value of error:

$$\epsilon = \frac{0.159 - 0.209}{0.209} * 100 = 23.9\%$$

Conclusion

The current measured by magnetic current sensors like the Rogowski coil or the Hall sensor can be affected by geometric parameters and surrounding magnetic fields. These errors can be mitigated by avoiding any type of geometric asymmetry in these sensors. The project covers different methods of estimating the error induced due to geometric asymmetry when the

position of the primary conductor is changed. The number of sensing elements in Hall sensor, number

of turns in Rogowski coil and the gap between windings in the coil can all impact on the magnitude of this error. We have estimated this error using analytical formula, finite element modelling and also measured this error with some physical experiments. The results from each of these methods are summarized in this table below

Table 4.1: Summary of results

	Analytical model		Finite element model		Experimental measurement	
	error	Induced voltage/ net flux	error	Induced voltage/ net flux	error	Induced voltage/ net flux
Hall sensor	-24.05%	6.25E-11 Wb	-35.80%	6.35E-12 Wb	-23.90%	0.209 V
Rogowski coil (single gap)	-2.02%	314.57 μv	-9.80%	301.58 μv	-1.51%	306.93 μv
split core coil	-1.77%	572.64 μv	10.20%	615.48 μv	1.87%	577 μv

From the above table we can see that the analytical model agrees well with the experimental results. However, the finite element model seems to overestimate the error and mostly underestimates the induced voltage and flux. The inaccuracy in the finite element model is probably because of improper generation of mesh. The software used for meshing (Ansys Maxwell) only allows us to add some basic meshing parameters which are not enough to create a mapped mesh. Meshing the model in some other meshing software and importing it to maxwell may yield better results.

References

- [1] S. GmbH, “Unidirectional Hall Effect DC Current Sensor CYHCT-C1TV, Output: 0-10 V DC, Power Supply: +24 V DC, Window: Ø 20 mm, Connector: Phoenix,” *Sonnecy Shop*. <https://www.sonnecy-shop.com/en/unidirectional-hall-effect-dc-current-sensor-cyhct-c1tv-output-0-10-v-dc-power-supply-24-v-dc-window-oe-20-mm-connector-phoenix.html> (accessed Aug. 21, 2023).
- [2] S. Kulkarni and D. Divan, “An Edge-Intelligent, Clip-on Rogowski Current Sensor With Wide Dynamic Range,” *IEEE Sensors J.*, vol. 21, no. 2, pp. 1059–1071, Jan. 2021, doi: [10.1109/JSEN.2019.2954273](https://doi.org/10.1109/JSEN.2019.2954273).
- [3] “Electric current. - Wikipedia.” https://en.wikipedia.org/wiki/Electric_current. (accessed Aug. 26, 2023).
- [4] M. Novák, L. Slavík, M. Blížkovský, and G. Cubreli, “Overview of principles for measuring el. Stream”.
- [5] *Introduction to magnetic current sensing*, (Mar. 16, 2020). Accessed: Aug. 26, 2023. [Online Video]. Available: <https://www.youtube.com/watch?v=qK5hDY4B0H8>
- [6] M. El-Shahat, E. Tag Eldin, N. A. Mohamed, A. EL-Morshedy, and M. E. Ibrahim, “Measurement of Power Frequency Current including Low- and High-Order Harmonics Using a Rogowski Coil,” *Sensors*, vol. 22, no. 11, p. 4220, Jun. 2022, doi: [10.3390/s22114220](https://doi.org/10.3390/s22114220).
- [7] “Lenz’s Law of Electromagnetic Induction: Definition & Formula | Electrical4U.” <https://www.electrical4u.com/lenz-law-of-electromagnetic-induction/> (accessed Aug. 26, 2023).
- [8] “A magnetic field due to a long straight wire carrying a current I is proportional to A . B . I^2 . C . I^3 . D . \sqrt{I} .” <https://www.vedantu.com/question-answer/a-magnetic-field-due-to-a-long-straight-wire-class-12-physics-cbse-5fb21ec0bb1ad308e51138d9> (accessed Aug. 26, 2023).
- [9] “Magnetic Permeability -Definition, Formula, SI Unit, Types, FAQs,” *BYJUS*. <https://byjus.com/jee/magnetic-permeability/> (accessed Aug. 26, 2023).
- [10] B. Djokić, “The Design and Calibration of Rogowski Coils,” *NCSLI Measure*, vol. 4, no. 2, pp. 62–75, Jun. 2009, doi: [10.1080/19315775.2009.11721474](https://doi.org/10.1080/19315775.2009.11721474).
- [11] J. N. Fritz, “A PCB Integrated Differential Rogowski Coil for Non-Intrusive Current Measurement Featuring High Bandwidth and dv/dt Immunity”.
- [12] M. Chiampi, G. Crotti, and A. Morando, “Evaluation of Flexible Rogowski Coil Performances in Power Frequency Applications,” *IEEE Trans. Instrum. Meas.*, vol. 60, no. 3, pp. 854–862, Mar. 2011, doi: [10.1109/TIM.2010.2060223](https://doi.org/10.1109/TIM.2010.2060223)
- [13] M. H. Hayes, *Schaum’s outline of theory and problems of digital signal processing*. in Schaum’s outline series. New York: McGraw Hill, 1999.
- [14] S. Tumanski, *Handbook of Magnetic Measurements*. Boca Raton: CRC Press, 2011. doi: [10.1201/b10979](https://doi.org/10.1201/b10979).

List of Attachments

File Name	Description
Data_Processing_Hall.m	Plots processed data for Hall sensor experiment.
Data_Processing_Rogowski_Coil.m	Plots processed data for Rogowski coil experiment.
Hall_Analysis_at_the_centre.aedtz	Finite element model to find flux through 4 given surfaces when conductor is in the centre.
Hall_Analysis_near_the_circumference.aedtz	Finite element model to find flux through 4 given surfaces when conductor is near the edge of the sensor hole.
Hall_data.mat	Measured and processed data for the Hall experiment.
Hall_direction_analysis.m	MATLAB script for analytical calculation of error for different directions of conductor displacement.
Hall_error_Calculation.m	MATLAB script for analytical calculation of error for different values of conductor displacement.
hall_net_flux.m	MATLAB script for analytical calculation of net flux when the conductor is outside the sensor hole.
Induced_voltage_PCB_coil.m	calculates the voltage induced due to an external current carrying wire placed near the gap. (single gap PCB coil)
Induced_Voltage_split_core.m	calculates the voltage induced due to an external current carrying wire placed near the gap. (split core coil)
Measuring_setup_hall.m	MATLAB script used to measure and process the data of the Hall experiment.
Measuring_setup_Rogowski.m	MATLAB script used to measure and process the data of the Rogowski coil experiments.
Merene_body_mesh2.m	MATLAB script used for setting different positions of primary conductor for Rogowski coil experiments
Merene_body_mesh4.m	MATLAB script used for setting different positions of primary conductor for Hall sensor experiments.
PCB_coil_conductor_in_the_centre.aedtz	finite element model of PCB coil with conductor in the centre.
PCB_coil_conductor_near_gap.aedtz	finite element model of PCB coil with conductor near the gap.
PCB_Coil_data.mat	Measured and processed data for the single gap coil experiment.
PCB_Coil_error_calc.m	MATLAB script for analytical calculation of error. (single gap coil)
Split_core_coil_Data.mat	Measured and processed data of split core coil experiment.
SPLIT_CORE_conductor_in_the_centre.aedtz	finite element model of split core coil with conductor in the centre
SPLIT_CORE_conductor_near_gap.aedtz	finite element model of split core coil with conductor near the gap.

Split_core_error_calc.m	MATLAB script for analytical calculation of error (split core coil).
-------------------------	--

Note: Due to size related constrains the ansys files are uploaded without the results, and some “.mat“ files are uploaded after downsampling the measured signal.